CALCULATION OF CROSS SECTIONS FOR ELASTIC SCATTERING OF ELECTRONS BY A MAGNESIUM ATOM AT INTERMEDIATE ENERGIES

By

KARIUKI PETER KINUTHIA
B. Ed (Sc)

I56/12353/04

A thesis is submitted in partial fulfillment of the requirements for the award of the degree of Master of Science in the School of Pure and Applied Sciences of Kenyatta University.

Department of Physics

November, 2009

DECLARATION

This thesis is my original work and has not been presented for award of a degree in any other University.

Kariuki Peter Kinuthia …… ……

Signature Date

We confirm that the candidate, under our supervision, carried out the work reported in this thesis.

Dr. C. S. Singh …… ……

Signature Date

Department of Physics

Kenyatta University

P.O BOX 43844

Nairobi, Kenya

Prof. J. Okumu …… ……

Signature Date

Department of Physics

Kenyatta University

P.O BOX 43844

Nairobi, Kenya

DEDICATION

This thesis is dedicated to my entire family for their unwavering support during this challenging period of my life.

ACKNOWLEDGEMENTS

I start by thanking our heavenly Father from whom all good things come. I am also grateful to my entire family for their moral and materials support especially my dear sister Lucy who made it possible for me to get learning materials which were very helpful in my research and coursework.

I thank the physics department, Kenyatta University, for admitting me to the Masters Degree Program. I thank the current Chairman, Dr Migwi, for his very useful advice throughout the course. I am extremely grateful to my Principle Supervisor, Dr Singh, for introducing me to the marvelous field of electron-atom collisions and the Co-supervisor Prof. Okumu for his input and material support. I would take this opportunity to also thank Dr Ambusso for introducing me to the wonderful art of computer programming.

I am grateful to my parents, the late Dominic Kariuki and my mom, Lois Njoki, for the physics genes. Finally I thank my lovely wife Annie and son Eugene for making this trying period of my life bearable!

TABLE OF CONTENTS

Chapter 6

Conclusions and Recommendations

LIST OF FIGURES

LIST OF TABLES

SYMBOLS

$f(\theta)$	Scattering amplitude
χ	Total wavefunction of the continuum electron
u_l	Radial wavefunction of the continuum electron
δ_l	Phase shift corresponding to u_l
σ_l	Integral cross section
H	Total Hamiltonian of the electron-atom system
H_T	Target atom Hamiltonian
E	Total energy of the electron-atom system
$E^{'}$	Energy of the continuum electron
Ψ	Total wavefunction of the electron-atom system
$\wp_{oi}$	Exchange operator
A	Antisymmetrization operator
V	Electron-atom interaction potential
V_{opt}	The optical potential
V_{st}	The static potential
V_{ex}	Exchange potential
V_{pol}	Polarization potential
V_{abs}	Absorption potential
K	Kinetic energy operator
k	Momentum of the continuum electron
k_F	Fermi momentum

Δ	Average excitation energy
Y_{lm}	Spherical harmonic
P_l	Legendre polynomial
$P_{n_a l_a}$	Radial wavefunction of target atom
Z	Atomic number of the target atom
N	Number of electrons in the target atom
j_l	Spherical Bessel function
n_l	Spherical Neumann function
V^{ad}	Adiabatic polarization potential
V_{se}	Static-exchange potential
$\rho(r)$	Electron-charge density

ABBREVIATIONS

OMP	Optical Model Potential Method
CC5	Five-State Coupled-Channels Method
CCO	Coupled-Channels Optical Method
XPS	X-ray Photoelectron Spectroscopy
AES	Auger-Electron Spectroscopy
DCS	Differential Cross Section
ICS	Integral Cross Section
CCC	Convergent Close Coupling Method

ABSTRACT

Elastic electron-atom collision data from experimental and theoretical studies is useful in the interpretation of spectra obtained in X-ray photoelectron spectroscopy and Auger electron spectroscopy as well as in the Monte Carlo simulation of conduction electrons in solids. In principle the behaviour of an electron-atom collision system is predicted by solving the Schrödinger equation. However this task is far from simple in that the equation can only be solved exactly for a two-body collision problem and consequently approximation methods are necessary for electron-atom scattering. In this study the Optical Model Potential method was used to calculate cross sections for elastic scattering of electrons by a magnesium atom at intermediate energies. Computer program PSCATT was developed to solve the Schrödinger equation numerically. Through use of a complex optical potential which accounts for possibility of inelastic processes at intermediate energies, the results obtained were found to be in fairly good agreement with recent measured results. The present results were also found to be comparable to, and in some cases better than, theoretical results obtained using sophisticated multi-channel methods. The computer program used in this study is much less demanding on computer power than the computer codes associated with multi-channel methods which has implications in terms of reducing research costs.

CHAPTER 1

INTRODUCTION

Background to the Study

Electron-atom scattering has played and continues to play an important role in the development of modern physics. The first electron-atom scattering experiments were performed in 1921 by Ramsauer who observed that the elastic scattering of low energy electrons, having incident energy ≈ 0.7 eV, by noble gas atoms was characterized by a marked transparency indicating the near absence of scattering. This was in contradiction with classical mechanics which predicts a monotonic increase in the number of scattered electrons as the incident–electron energy decreases. Numerous scattering experiments have since been performed at a wide range of scattering energies, for a variety of target atoms and for both elastic and inelastic processes. These experiments include the recent measurements by Predojevic *et al*. (2007) on elastic electron-magnesium scattering.

A typical set-up for electron-atom scattering experiments is illustrated in figure 1.1 (McCarthy and Weigold, 1995). A collimated beam of mono-energetic electrons having momentum $\vec{k}$ is incident on target atoms. Initially, the incident electrons which approach from infinity, on an atomic scale, do not interact with the target atoms. However, when the electrons are in the vicinity of the target atoms interaction occurs. The incident electrons may then be deflected from their initial path without losing or gaining energy. This situation corresponds to elastic scattering. In case the incident electrons have sufficient energy, they may excite or even ionize the target atoms resulting in loss of energy and the electrons are then inelastically scattered. In the intermediate energy

region, the incident electrons have sufficient energy to not only excite the target atoms but also ionize the atoms. The scattered electrons are detected at infinity from the interaction region. These electrons have final momentum $\vec{k}'$.

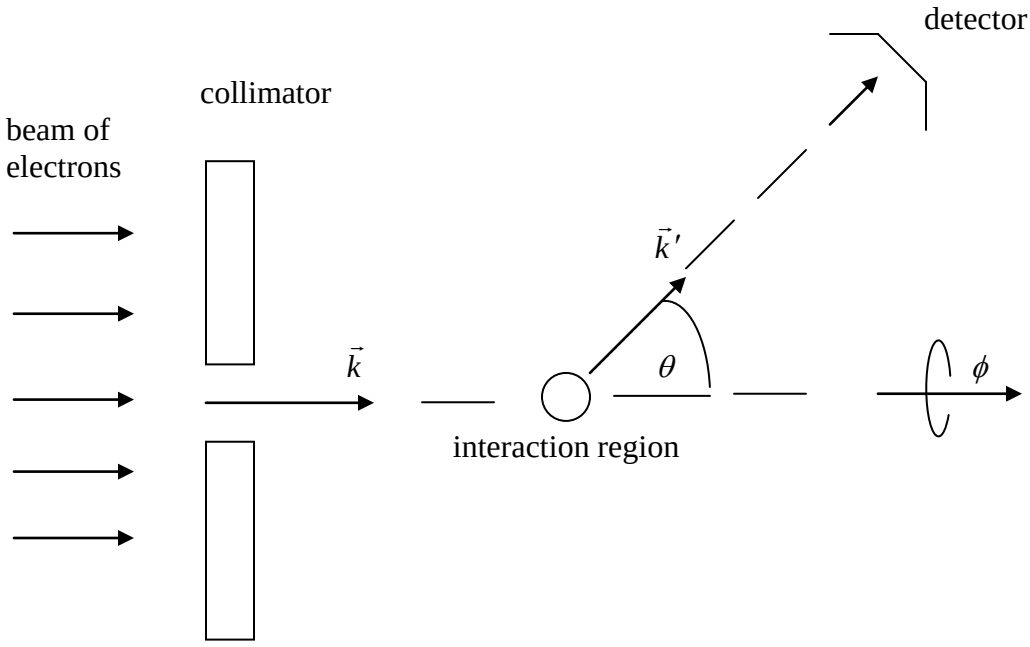

Figure 1.1. A schematic diagram of a scattering experiment.

The polar and azimuthal angles θ and ϕ, respectively, give the direction of $\vec{k}'$ relative to $\vec{k}$. Electron-atom scattering experiments yield differential cross section (DCS) results. The differential cross section is a measure of the probability that electrons will be scattered in a given direction specified by θ and ϕ. Other cross sections such as the integral cross section (ICS) may be calculated from differential cross section results.

The availability of measured electron-atom scattering data has given a strong impetus to the development of theoretical quantum-mechanical approaches that can accurately

predict differential and integral cross sections. The aim of electron-atom scattering theory is to model as accurately as possible the behavior of the electron-atom system in the interaction region. A number of theoretical methods have been developed for calculation of cross sections including the distorted-wave Born approximation, DWBA, (Joachain**,** 1975), the close-coupling, CC, method (McCarthy and Weigold, 1995) and the R-matrix method (Burke and Berrington, 1993). In the DWBA method the continuum wave function of the incident electron is calculated using the ground state average of the electron-atom interaction potential and the wave function of the scattered electron calculated using the excited state average potential. In the CC method, the electron-atom wavefunction is expanded in terms of known target-atom states and unknown scattered-electron states. In the R-matrix approach, the electron-atom system is treated as a compound system using atomic-structure theory. These three methods are usually applied to inelastic scattering for calculating the probability for transition of the target atoms from the initial state to the final state.

For elastic scattering, the most straightforward approach to calculation of cross sections is the optical model potential, OMP, method (Joachain, 1975). This approach reduces the many-body problem of electron-atom scattering to a one-body problem involving movement of incident electrons in a complex potential. The real part of the potential accounts for the electron-atom Coulomb interaction, the Pauli exclusion effects and polarization of the target atom by the incident electrons. The imaginary part known as the absorption potential, takes into account the possibility of inelastic scattering at intermediate energies. Once the optical potential has been formulated Schrödinger’s

equation is solved subject to certain physical boundary conditions and the solution used to calculate differential and integral cross sections.

In general, the comparison of measured and calculated cross sections is first and foremost important in the understanding of the nature of interactions of electrons with atoms. Cross sections for electron-atom inelastic scattering are important in laser development and in plasma physics (McCarthy and Weigold, 1995). Elastic scattering cross sections are useful in X-ray photoelectron spectroscopy, XPS, and Auger-electron spectroscopy, AES, (Jablonski *et al*., 2004) where the signal electrons are elastically scattered from within metal surfaces. Elastic scattering cross sections also provide vital input in the Monte-Carlo simulation of conduction of electrons in solids (Jablonski *et al*., 2004).

1.2 Statement of Research Problem

In this study differential and integral cross sections for elastic scattering of electrons by a magnesium atom in the intermediate energy region were calculated using the optical model potential method. Recently, Predojevic *et al*. (2007) have reported experimental differential and integral cross sections for elastic electron-magnesium scattering at intermediate energies. These latest results are inconsistent with the earlier results by Williams and Trajmar (1978) and although various theoretical approaches including the Close-Coupling, R-Matrix and Optical Model potential methods have been applied to the problem of elastic electron-magnesium scattering, exact agreement among these theoretical approaches and between theory and experiment is generally lacking which makes further work on the problem necessary.

1.3 Rationale of the Study

The Optical Model Potential (OMP) method has been applied by Khare *et al*. (1983) and Yousif and Lennart (2002) to the problem of elastic scattering of electrons by magnesium atom at intermediate energies. However both studies used a real potential which did not include the imaginary part of the optical potential referred to as the absorption potential, which accounts for the possibility of excitation and ionization of the atom at intermediate energies. In this study a complex optical potential which included the absorption potential proposed by Staszewska *et al*. (1984) was used in order to account for inelastic processes.

1.4 Objectives

1.4.1 Main Objective

The main objective was to calculate cross sections for elastic scattering of electrons by magnesium atom at intermediate energies.

1.4.2 Specific Objectives

(i) To formulate a suitable complex optical potential.

(ii) To calculate differential cross sections (DCS) and integral cross sections (ICS) at electron impact energies 10, 15, 20, 40, 60, 80 and 100 eV.

CHAPTER 2

LITERATURE REVIEW

Over the last three decades several experimental and theoretical differential cross sections for elastic electron-magnesium scattering at intermediate energies have been reported. While earlier experiments were limited to the lower end of the intermediate energy range, recent experimental data covers the entire range from 10 – 100 eV. The first calculated results were obtained using the Optical Model Potential method. Later the multi-channel five-state Close Coupling method was applied to the problem. Recently the more sophisticated Convergent Close Coupling and R-Matrix multi-channel methods have been used. The measured and calculated results so far reported are discussed in sections 2.1, 2.2 and 2.3 of this chapter.

2.1 Experimental Differential Cross Sections

The earliest experimental DCS results for elastic scattering of electrons by magnesium are those of Williams and Trajmar (1978) who measured DCS values at electron impact energies 10, 20 and 40 eV over scattering angle from 10° to130°. Brown *et al*. (2003) measured relative (unnormalized) DCS values at electron impact energy 40 eV from 10° to140°. Later, Brown *et al.* (2005) measured relative DCS values at 20 eV from 10° to140°. Recently Predojevic *et al*. (2007) have reported DCS results at electron impact energies 10, 15, 20, 40, 60, 80 and 100 eV from 10° to150°.

Compared to the results of Williams and Trajmar (1978), the recent DCS results by Predojevic *et al.* (2007) are lower at 10 eV and 20 eV over all scattering angles but are

higher at 40 eV. When the relative results of Brown *et al*. (2003) at 40 eV are renormalized to the results of Predojevic *et al*. (2007), they are found to be in excellent agreement over all scattering angles. The results of Brown *et al*. (2003) are not absolute and their usefulness is limited to comparison with other measured results. The renormalized experimental results of Brown *et al.* (2005) at 20 eV compare fairly well with those of Predojevic *et al*. (2007). There are no experimental DCS results at 15, 60, 80 and 100 eV to compare with the results of Predojevic *et al*. (2007).

2.2 Close Coupling and R-Matrix Methods

Several close coupling calculations have been applied to the problem of elastic scattering of electrons by a magnesium atom. Mitroy and McCarthy (1989) carried out a five-state close coupling (CC5) calculation at 10, 20, 40 and 100 eV. The calculations yielded DCS results lower than the measured results of Williams and Trajmar (1978) at 10 and 20 eV at all scattering angles but were higher than the measured results at 40 eV at all angles. The CC5 results are in close agreement with the measured results of Predojevic *et al.* (2007) at 10 and 20 eV at scattering angles $\leq 120^{\circ}$ but differ significantly for larger angles. At 40 eV the agreement is very good at all scattering angles. However, at 100 eV the CC5 results are appreciably higher than the results of Predojevic *et al*. (2007) at scattering angles $> 30^{\circ}$.

McCarthy *et al*. (1989) carried out a six-state coupled channels optical (CCO6) calculation at 10, 20 and 40 eV. The results are significantly lower than the measured results of Williams and Trajmar (1978) at 10 and 20 eV at scattering angles $> 20^{\circ}$ but are

higher than the measured results at 40 eV. There is close agreement between the CCO6 results and the measured results of Predojevic *et al*. (2007) at 10, 20 and 40 eV at scattering angles $\leq 40^{\circ}$ but at higher angles the CCO6 results are generally lower than the measured results. The CCO6 results are in close agreement with the CC5 results of Mitroy and McCarthy (1989) at scattering angles up to about 50° at 10, 20 and 40 eV but at larger angles the CCO6 results are lower than the CC5 results.

Brown *et al*. (2003) reported convergent close coupling (CCC) results at 40 eV. These results are higher than the experimental results of Williams and Trajmar (1978) at scattering angles $\geq 40^{\circ}$. However, at 40 eV the CCC results are in excellent agreement with the experimental results of Predojevic *et al*. (2007) at all scattering angles. The CCC results are also in very good agreement with the CC5 results of Mitroy and McCarthy (1989) at all scattering angles but are higher than the CCO6 results of McCarthy *et al.* (1989) at scattering angles $> 30^{\circ}$.

Brown *et al.* (2005) reported CCC and R-Matrix with Pseudo-State (RMPS) differential cross section results at 20 eV. These two calculations are in close agreement with each other but the minimum at $\approx 50^{\circ}$ is much deeper in the RMPS than in the CCC calculation. The CCC and RMPS results are higher than the experimental results of Williams and Trajmar (1978) at 20 eV at all scattering angles. The CCC results are however in good agreement with the measured results of Predojevic *et al*. (2007) but the two minima in the CCC results at 50° and 130° are appreciably deeper than the corresponding minima in the results of Predojevic *et al*. (2007).

2.3 Optical Model Potential Method

Two variants of the optical model potential method have been applied to elastic scattering of electrons by a magnesium atom. Khare *et al*. (1983) used a real optical potential consisting of a static potential, the exchange potential of Vanderpoorten (1975) and a semi-empirical polarization potential. Yousif and Lennart (2002) used a real optical potential consisting of a static potential, Hara exchange potential and a Hedin-Lundqvist polarization potential.

The differential cross section results of Khare *et al*. (1983) at 10 and 20 eV are higher than the experimental results of Williams and Trajmar (1978) at scattering angles up to $\approx 100^{\circ}$ but are lower than the measured results at angles between 130° and 160°. At larger scattering angles the results of Khare *et al*. (1983) are higher than the extrapolated results of Williams and Trajmar (1978). At 40 eV the results of Khare *et al.* (1983) are higher than the measured results of Williams and Trajmar (1978) at all scattering angles. Compared to the measured results of Predojevic *et al*. (2007) the results of Khare *et al*. (1983) are higher at 10 eV at all scattering angles. At 20 eV the results of Khare *et al*. (1983) are higher at scattering angles up to $\approx 100^{\circ}$ but are lower between 110° and 130° and are again higher at angles $> 130^{\circ}$. At 40 and 100 eV the results of Khare *et al*. (1983) are in close agreement with the experimental results of Predojevic *et al*. (2007) at scattering angles $< 30^{\circ}$ but are higher than the measured results at larger scattering angles.

At 10 eV the optical model potential results of Yousif and Lennart (2002) are higher than the measured results of Williams and Trajmar (1978) at scattering angles between 30° and 120° but are lower at scattering angles $< 30^\circ$ and at angles $> 120^\circ$. At 20 eV the differential cross section results of Yousif and Lennart (2002) are close to the experimental results of Williams and Trajmar (1978) at all scattering angles. At 40 eV the results of Yousif and Lennart (2002) are lower than the results of Williams and Trajmar (1978) at scattering angles $< 10^\circ$ but are higher at larger scattering angles. The optical model potential results of Yousif and Lennart (2002) and those of Khare *et al.* (1983) agree particularly well with the CC5 results of Mitroy and McCarthy (1989) at 40 and 100 eV at most scattering angles but not at 10 and 20 eV where they are appreciably higher than the CC5 results.

In this study a complex optical potential, consisting of a static potential, an exchange potential (Furness and McCarthy, 1973: Gianturco and Scialla, 1987), a non-adiabatic (energy-dependent) polarization potential (Valone *et al.*, 1982) incorporating an adiabatic polarization potential (Eades *et al.*, 1982) and an absorption potential (Staszewska *et al.*, 1984), was used. As noted in the previous chapter this potential takes into consideration inelastic processes that occur in electron-magnesium scattering at intermediate energies. The potential used in this study is an improvement over the real potentials used by Khare *et al.* (1983) and Yousif and Lennart (2002). Consequently the present DCS results are in better agreement with the recent measured results of Predojevic *et al.* (2007). The complex optical potential is discussed further in chapter 3.

CHAPTER 3

THEORY

In sections 3.1 and 3.2 of this chapter, the formal optical potential is obtained in the close-coupling formalism in which the state describing the electron-atom system is expanded in terms of known electron-atom channel states and unknown radial wavefuntions of the scattered electron. One desirable feature of this approach is that the exchange term, as well as the static term in the optical potential, is obtained in a straight forward manner. This derivation of the optical potential follows closely the work of Furness and McCarthy (1973), Bartschat *et al*. (1988) and McEachran (1996). In section 3.3, the static, exchange, polarization and absorption terms in the optical potential are presented in computational form. In section 3.4, the radial wavefunctions of the ground state of magnesium atom used in this study are given. Finally in section 3.5, the manner in which observables in the form of differential and integral cross sections are calculated from the theory to yield results that can be compared directly with experimentally determined values is discussed. All quantities in this chapter are in atomic units $(\hbar = m_e = e = 1)$.

3.1 The Close-Coupling Expansion

The scattering of an electron by an atom is a many-body problem. Consider an electron incident on a neutral atom having Z protons and $N = Z$ electrons. The time-independent Schrödinger equation governing this electron-atom system having total energy E is

$$(H - E)\Psi = 0 . \tag{3.1}$$

The total Hamiltonian H of the system can be expressed as

$$H = K + H_T + V . \tag{3.2}$$

In this expression

$$K = -\frac{1}{2}\nabla^2 \tag{3.3}$$

is the kinetic energy operator,

$$H_T = \sum_{i=1}^{N}\left(-\frac{1}{2}\nabla_i^2 - \frac{Z}{r_i}\right) + \frac{1}{2}\sum_{i\neq j}\frac{1}{\left|\vec{r}_i - \vec{r}_j\right|} \tag{3.4}$$

is the target-atom Hamiltonian and

$$V = -\frac{Z}{r} + \sum_{i=1}^{N}\frac{1}{\left|\vec{r}_i - \vec{r}\right|} \tag{3.5}$$

is the electron-atom interaction potential.

Introducing the *N*-electron target wavefunctions Φ_j which diagonalize the target Hamiltonian according to

$$\left\langle \Phi_i \middle| H_T \middle| \Phi_j \right\rangle = \varepsilon_j \delta_{ij} , \tag{3.6}$$

where ε_j is the energy of the *j*th target state, we may write the total wavefunction for the system in terms of channel wavefunctions $\overline{\Phi}_j{}^{LS\Pi}$ and radial scattering wavefunctions F_j using the close-coupling expansion

$$\Psi = \mathrm{A}\sum_j \overline{\Phi}_j{}^{LS\Pi}\frac{1}{r}F_j(r). \tag{3.7}$$

The channel functions $\overline{\Phi}_j{}^{LS\Pi}$ are obtained by coupling the target wavefunctions Φ_j to the angular and spin wavefunctions of the projectile electron to obtain functions having

definite total angular momentum L, total spin S and total parity Π. In equation (3.7) the summation is over all discrete and continuum target states and A is the antisymmetrization operator (Joachain, 1975) given apart from a normalization factor by

$$\mathrm{A} = \mathrm{I} - \sum_{i=1}^{N} \wp_{0i} \,. \tag{3.8}$$

In equation (3.8) $\wp_{0i}$ is the exchange operator which interchanges the *i*th target electron and the projectile (zeroth) electron. The operator A in equation (3.7) is needed to fulfill the Pauli Exclusion Principle in the description of the $(N+1)$ -electron system.

Writing $\mathrm{A} = 1 + (\mathrm{A} - 1)$, (3.7) becomes

$$\Psi = \sum_j \overline{\Phi}_j \frac{1}{r} F_j(r) + \sum_j (\mathrm{A}-1)\overline{\Phi}_j \frac{1}{r} F_j(r). \tag{3.9}$$

Substituting equations (3.2) and (3.9) into (3.1) we have

$$(K + H_T + V - E)\left[\sum_j \overline{\Phi}_j \frac{1}{r} F_j(r) + \sum_j (\mathrm{A}-1)\overline{\Phi}_j \frac{1}{r} F_j(r)\right] = 0 \,. \tag{3.10}$$

Premultiplying (3.10) by $\left\langle \overline{\Phi}_i \right|$ we obtain

$$\sum_j \left\langle \overline{\Phi}_i \middle| K + H_T + V - E \middle| \overline{\Phi}_j \frac{1}{r} F_j(r) \right\rangle$$

$$+ \sum_j \left\langle \overline{\Phi}_i \middle| K + H_T + V - E \middle| (\mathrm{A}-1)\overline{\Phi}_j \frac{1}{r} F_j(r) \right\rangle = 0 \,. \tag{3.11}$$

Using equation (3.3) as well as

$$\left\langle \overline{\Phi}_i \middle| H_T = \left\langle \overline{\Phi}_i \right| \varepsilon_i \tag{3.12}$$

and writing $$E-\varepsilon_i=\frac{1}{2}k_i^{\,2} \tag{3.13}$$

where $k_i^{\,2}/2$ is the energy of the projectile electron in the *i*th channel, we can simplify equation (3.11) to

$$\sum_j\left\langle\overline{\Phi}_i\left|-\frac{1}{2}\nabla^2+V-\frac{1}{2}k_i^{\,2}\right|\overline{\Phi}_j\frac{1}{r}F_j(r)\right\rangle$$

$$+\sum_j\left\langle\overline{\Phi}_i\left|-\frac{1}{2}\nabla^2+V-\frac{1}{2}k_i^{\,2}\right|(\mathrm{A}-1)\overline{\Phi}_j\frac{1}{r}F_j(r)\right\rangle=0. \tag{3.14}$$

Expressing the Laplacian operator in (3.14) in spherical coordinates we have (McEachran, 1996)

$$\sum_j\left\langle\overline{\Phi}_i\left|\frac{d^2}{dr^2}-\frac{l_j(l_j+1)}{r^2}-2V+k_i^{\,2}\right|\overline{\Phi}_j\frac{1}{r}F_j(r)\right\rangle$$

$$+\sum_j\left\langle\overline{\Phi}_i\left|\frac{d^2}{dr^2}-\frac{l_j(l_j+1)}{r^2}-2V+k_i^{\,2}\right|(\mathrm{A}-1)\overline{\Phi}_j\frac{1}{r}F_j(r)\right\rangle=0. \tag{3.15}$$

Finally using $$\left\langle\overline{\Phi}_i\left|\overline{\Phi}_jF_j\right\rangle=F_j\delta_{ij}, \tag{3.16}$$

and assuming that the overlap integrals involving bound and continuum wavefunctions are equal to zero (Furness and McCarthy, 1973) we set

$$\left\langle\overline{\Phi}_i\left|(\mathrm{A}-1)\overline{\Phi}_jF_j\right\rangle=0, \tag{3.17}$$

to obtain the following set of coupled integro-differential equations for the channel radial functions $F_i(r)$ of the scattered electron (Bartschat *et al.*, 1988)

$$\left(\frac{d^2}{dr^2}-\frac{l_i(l_i+1)}{r^2}+k_i^{\,2}\right)F_i(r)=2\sum_jV_{ij}F_j(r)+2\sum_jW_{ij}F_j(r), \tag{3.18}$$

where the direct and exchange potential terms are given respectively by

$$V_{ij} = -\frac{Z}{r}\delta_{ij} + \left\langle \overline{\Phi}_i \left| \sum_{k=1}^{N} \frac{1}{|\vec{r}_k - \vec{r}|} \right| \overline{\Phi}_j \right\rangle \tag{3.19}$$

and

$$W_{ij}F_j(r) = \left\langle \overline{\Phi}_i \left| \sum_{k=1}^{N} \frac{1}{|\vec{r}_k - \vec{r}|} \right| (\mathrm{A}-1)\overline{\Phi}_j F_j(r) \right\rangle. \tag{3.20}$$

3.2 The Formal Optical Potential

Since we are interested in elastic scattering of an electron from the ground state Φ_0 of a neutral atom, we specialize (3.18) to the elastic channel by setting $i = 0$ to obtain

$$\left(\frac{d^2}{dr^2} - \frac{l(l+1)}{r^2} + k^2 \right) u_l(r) = 2V_{00}u_l(r) + 2W_{00}u_l(r) + 2\sum_{j\neq 0} V_{0j}(r)F_j(r), \tag{3.21}$$

where the exchange terms W_{0j} for $j > 0$ have been neglected and we have set $F_0(r) = u_l(r)$. In order to obtain an expression for the radial functions $F_j(j \neq 0)$, (3.18) is again specialized to scattering from the *j*th excited target state Φ_j to get (Bartschat *et al.*, 1988)

$$\left(\frac{d^2}{dr^2} - \frac{l_j(l_j+1)}{r^2} + k_j{}^2 \right) F_j(r) = 2V_{j0}u_l(r), \tag{3.22}$$

The solution to this inhomogeneous equation is (Chattopadhyay, 1990)

$$F_j(r) = 2\int_0^\infty dr' G_j{}^+(k_j; r, r') V_{j0}(r') u_l(r'), \tag{3.23}$$

where $G_j{}^+(k_j; r, r')$ is the complex free-particle Green's function corresponding to the *j*th channel state. This satisfies outgoing wave boundary conditions (as indicated by the superscripts) and is given in terms of Ricatti-Bessel functions f_{l_j} and g_{l_j} as

$$G_j^{+}(k_j;r,r') = \frac{1}{k_j} f_{l_j}(k_j r_<)\left[g_{l_j}(k_j r_>) + i f_{l_j}(k_j r_>)\right]. \tag{3.24}$$

Using equation (3.23) in (3.21) we have

$$\left(\frac{d^2}{dr^2} - \frac{l(l+1)}{r^2} + k^2\right)u_l(r) = 2V_{00}u_l(r) + 2W_{00}u_l(r) + 4\sum_{j\neq 0}\int_0^\infty dr' V_{0j}(r) G_j^{+}(k_j;r,r') V_{j0}(r') u_l(r'). \tag{3.25}$$

Equation (3.25) can be written compactly as

$$\left(\frac{d^2}{dr^2} - \frac{l(l+1)}{r^2} + k^2 - 2V_{opt}\right)u_l(r) = 0, \tag{3.26}$$

where we have defined the complex non-local optical potential operator V_{opt} such that

$$V_{opt}u_l(r) = V_{00}u_l(r) + W_{00}u_l(r) + 2\sum_{j\neq 0}\int_0^\infty dr' V_{0j}(r) G_j^{+}(k_j;r,r') V_{j0}(r') u_l(r'). \tag{3.27}$$

In the optical potential V_{00} is the static potential which results from the Coulomb interaction between the projectile electron and the nucleus as well as electrons of the target atom, W_{00} is the non-local exchange operator which accounts for the indistiguishability of the projectile and target electrons while the last term which has both imaginary and real parts accounts for virtual and real excitations as well as ionization of the target atom by the projectile electron.

In obtaining (3.26) from (3.1), the many-body problem of elastic scattering of an electron by a neutral atom has been effectively reduced to a one-body problem involving an electron of energy $E' = k^2/2$ moving in a non-local complex optical potential V_{opt}. In the

optical potential both the static and exchange potentials may be evaluated exactly but for ease of solution of equation (3.26) it is convenient to approximate the non-local exchange potential by a local potential. We also note that the third term in the optical potential is complicated to evaluate due to its non-local and complex nature and is usually approximated by a complex local potential the real part of which is a polarization potential V_{pol} used to account for polarization of the target atom charge cloud by the projectile electron while the imaginary part is an absorption potential V_{abs} which accounts for the possibility of inelastic scattering at intermediate energies.

3.3 Evaluation of the Optical Potential

In this section we evaluate the optical potential for elastic scattering of electrons by a neutral atom. The static potential is evaluated exactly while the non-local exchange potential operator is approximated by a local exchange potential following the method originally proposed by Furness and McCarthy (1973) and later refined by Gianturco and Scialla (1987). The real part of the third complex and non-local term of the optical potential is approximated by the polarization potential of Valone *et al.* (1982) and the imaginary part is approximated as the quasi-free absorption potential of Staszewska *et al*. (1984).

3.3.1 The Static Potential

From equation. (3.19) the static potential is given by

$$V_{st} = V_{00} = -\frac{Z}{r} + \left\langle \overline{\Phi}_0 \left| \sum_{i=1}^{N} \frac{1}{|\vec{r}_i - \vec{r}|} \right| \overline{\Phi}_0 \right\rangle. \qquad (3.28)$$

For an atom in a ^1S ground state the atomic state Φ_0 is coupled to the angular function $Y_{lm}(\hat{r})$ and spin function $\chi_{ms}(\sigma)$ of the scattered electron to yield a channel function $\overline{\Phi}_0{}^{LS}$ having definite total angular momentum *L* and spin *S* (McEachran, 1996)

$$\overline{\Phi}_0 = \sum_{mm_s} C(0lL;0mM_L)\, C(0\tfrac{1}{2}S;0m_sM_S)\, \Phi_0 Y_{lm}(\hat{r})\chi_{m_s}(\sigma), \tag{3.29}$$

where $C(j_1 j_2 j; m_1 m_2 m)$ is a Clebsch-Gordan coefficient. From (3.29), the second term in (3.28) becomes

$$\begin{aligned}\left\langle \overline{\Phi}_0 \left| \sum_{i=1}^{N} \frac{1}{|\vec{r}_i - \vec{r}|} \right| \overline{\Phi}_0 \right\rangle = & \sum_{mm_s m' m_s'} C(0lL;0mM_L) C\left(0l'L';0m'M_L'\right) \\ & \times C(0\tfrac{1}{2}S;0m_sM_S) C\left(0\tfrac{1}{2}S';0m_s'M_S'\right) \\ & \times \left\langle \Phi_0 Y_{l'm'}(\hat{r})\chi_{m_s'}(\sigma) \left| \sum_{i=1}^{N} \frac{1}{|\vec{r}_i - \vec{r}|} \right| \Phi_0 Y_{lm}(\hat{r})\chi_{m_s}(\sigma) \right\rangle \delta_{ll'mm'} \delta_{mm_s'}\end{aligned} \tag{3.30}$$

From the well known identity for Clebsch-Gordan coefficients (Cowan, 1981)

$$\sum_{m_1 m_2} C(j_1 j_2 j; m_1 m_2 m) C(j_1 j_2 j'; m_1 m_2 m') = \delta_{jj'mm'}, \tag{3.31}$$

equation (3.30) becomes

$$\left\langle \overline{\Phi}_0 \left| \sum_{i=1}^{N} \frac{1}{|\vec{r}_i - \vec{r}|} \right| \overline{\Phi}_0 \right\rangle = \left\langle \Phi_0 Y_{lm}(\hat{r}) \left| \sum_{i=1}^{N} \frac{1}{|\vec{r}_i - \vec{r}|} \right| Y_{lm}(\hat{r}) \Phi_0 \right\rangle \delta_{LL'M_L M_L'} \delta_{SS'M_S M_S'}. \tag{3.32}$$

We now take the target ground state Φ_0 to be a properly anti-symmetrized Slater determinant of single-electron wavefunctions $\varphi_a(\vec{r})$ given by

$$\varphi_a(\vec{r}) = \frac{1}{r} P_{n_a l_a}(r) Y_{l_a m_a}(\hat{r}) \chi_{\mu_a}(\sigma). \tag{3.33}$$

Applying the rules for evaluation of matrix elements of one-electron operators between Slater determinants (Cowan, 1981), equation (3.32) reduces to

$$\left\langle \overline{\Phi}_0 \left| \sum_{i=1}^{N} \frac{1}{\left|\vec{r}_i - \vec{r}\right|} \right| \overline{\Phi}_0 \right\rangle = \sum_{n_a l_a m_a \mu_a} \left\langle \varphi_a(\vec{r}\,') Y_{l_a m_a}(\hat{r}) \left| \frac{1}{\left|\vec{r}\,' - \vec{r}\right|} \right| Y_{l_a m_a}(\hat{r}) \varphi_a(\vec{r}\,') \right\rangle, \tag{3.34}$$

where the summation on the RHS of (3.34) is over the single electron wavefunctions $\varphi_a(\vec{r})$. Expanding the inter-electronic distance in (3.34) in terms of renormalized spherical harmonics $C_\eta^\lambda(\hat{r})$ thus

$$\frac{1}{\left|\vec{r}\,' - \vec{r}\right|} = \sum_{\lambda\eta} (-1)^\eta \frac{r_<^{\ \lambda}}{r_>^{\lambda+1}} C_\eta^\lambda(\hat{r}) C_{-\eta}^\lambda(\hat{r}'), \tag{3.35}$$

where

$$C_\eta^\lambda(\hat{r}) = \left(\frac{4\pi}{2\lambda+1}\right)^{\frac{1}{2}} Y_{\lambda\eta}(\hat{r}), \tag{3.36}$$

equation (3.34) become

$$\left\langle \overline{\Phi}_0 \left| \sum_{i=1}^{N} \frac{1}{\left|\vec{r}_i - \vec{r}\right|} \right| \overline{\Phi}_0 \right\rangle = 2 \sum_{n_a l_a m_a} \sum_{\lambda\eta} (-1)^\eta \int d\hat{r} Y_{lm}^*(\hat{r}) C_{-\eta}^\lambda(\hat{r}) Y_{lm}(\hat{r})$$

$$\times \int_0^\infty dr' \frac{r_<^{\ \lambda}}{r_>^{\lambda+1}} P_{n_a l_a}^2(r') \int d\hat{r}' Y_{l_a m_a}^*(\hat{r}') C_\eta^\lambda(\hat{r}') Y_{l_a m_a}(\hat{r}'), \tag{3.37}$$

where we have summed over μ_a to obtain the factor 2 thus

$$\sum_{\mu_a = -\frac{1}{2}}^{+\frac{1}{2}} \chi_{\mu_a}^+(\sigma') \chi_{\mu_a}(\sigma') = 2\,. \tag{3.38}$$

Now using the Wigner-Eckart theorem (Cowan, 1981)

$$\left\langle lm\left|C_q^k\right|l'm'\right\rangle = (-1)^{l-m}\begin{pmatrix} l & k & l' \\ -m & q & m' \end{pmatrix}\begin{pmatrix} l & k & l' \\ 0 & 0 & 0 \end{pmatrix}, \tag{3.39}$$

the third integral in (3.37) may be evaluated in terms of 3-j symbols and to yield

$$\int d\hat{r}' Y^*_{l_a m_a}(\hat{r}') C^{\lambda}_{\eta}(\hat{r}') Y_{l_a m_a}(\hat{r}') = (-1)^{l_a - m_a}\begin{pmatrix} l_a & \lambda & l_a \\ -m_a & \eta & m_a \end{pmatrix}\begin{pmatrix} l_a & \lambda & l_a \\ 0 & 0 & 0 \end{pmatrix}\delta_{\eta 0}. \tag{3.40}$$

Summing this result over m_a we have

$$\sum_{m_a=-l_a}^{l_a}(-1)^{l_a-m_a}\begin{pmatrix} l_a & \lambda & l_a \\ -m_a & \eta & m_a \end{pmatrix} = \delta_{\lambda 0}(2l_a+1)^{1/2}, \tag{3.41}$$

and using the identity (Cowan, 1981)

$$\begin{pmatrix} l_a & 0 & l_a \\ 0 & 0 & 0 \end{pmatrix} = (2l_a+1)^{-1/2}, \tag{3.42}$$

equation (3.37) becomes

$$\left\langle \overline{\Phi}_0 \left| \sum_{i=1}^{N} \frac{1}{|\vec{r}_i - \vec{r}|} \right| \overline{\Phi}_0 \right\rangle = \sum_{n_a l_a} 2(2l_a+1)\int_0^{\infty} dr' \frac{P^2_{n_a l_a}(r')}{r_>}. \tag{3.43}$$

Finally using (3.43) in (3.28) we arrive at the expression for the static potential

$$V_{st}(r) = -\frac{Z}{r} + \sum_{n_a l_a} v_a \int_0^{\infty} dr' \frac{P^2_{n_a l_a}(r')}{r_>}, \tag{3.44}$$

where $v_a = 2(2l_a+1)$ is the occupation number of the $n_a l_a$ target subshell.

3.3.2 The Exchange Potential

From equation (3.20), the exchange potential is defined such that

$$V_{ex}u_l(r) \equiv W_{00}F_0(r) = \left\langle \overline{\Phi}_0 \left| \sum_{k=1}^{N} \frac{1}{|\vec{r}_k - \vec{r}|} \right| (\mathrm{A}-1)\overline{\Phi}_0 u_l(r) \right\rangle. \tag{3.45}$$

Using (3.8) this becomes

$$V_{ex}u_l(r) = -\left\langle \overline{\Phi}_0 \left| \sum_{k=1}^{N} \frac{1}{|\vec{r}_k - \vec{r}|} \right| \wp_{0i} \overline{\Phi}_0 u_l(r) \right\rangle . \tag{3.46}$$

Again for a determinantal target wavefunction Φ_0, we obtain after applying equation (3.29)

$$\begin{aligned} V_{ex}u_l(r) = & - \sum_{mm_s m' m_s'} C(0lL;0mM_L) C(0l'L';0m'M_{L'}) \\ & \times C(0\tfrac{1}{2}S;0m_s M_S) C(0\tfrac{1}{2}S';0m_s' M_S') \\ & \times \sum_{n_a l_a m_a \mu_a} \delta_{\mu_a m_s} \frac{1}{r} P_{n_a l_a}(r) \delta_{ll'mm'} \delta_{m_s m_s'} \\ & \times \left\{ \left\langle \varphi_a(\vec{r}\,') Y_{lm}(\hat{r}) \left| \frac{1}{|\vec{r}\,' - \vec{r}|} \right| Y_{l_a m_a}(\hat{r}) R_l(\vec{r}\,') \right\rangle \right\}, \end{aligned} \tag{3.47}$$

where we have defined

$$R_l(\vec{r}\,') = u_l(r) Y_{lm}(\hat{r}). \tag{3.48}$$

Using equation (3.31) we again obtain

$$\begin{aligned} V_{ex}u_l(r) &= -\delta_{LL'M_L M_L'} \delta_{SS'M_S M_S'} \sum_{n_a l_a m_a} \frac{1}{r} P_{n_a l_a}(r) \left\{ \left\langle \varphi_a(\vec{r}\,') Y_{lm}(\hat{r}) \left| \frac{1}{|\vec{r}\,' - \vec{r}|} \right| Y_{l_a m_a}(\hat{r}) R_l(\vec{r}\,') \right\rangle \right\} \\ &= -\sum_{n_a l_a m_a} \frac{1}{r} P_{n_a l_a}(r) \int d\hat{r} Y_{lm}^*(\hat{r}) Y_{l_a m_a}(\hat{r}) \int d^3 r' \varphi_a^*(\vec{r}\,') \frac{1}{|\vec{r}\,' - \vec{r}|} R_l(\vec{r}\,'). \end{aligned} \tag{3.49}$$

The second integral in (3.49) may be carried out approximately resulting in a local exchange potential as described by Furness and McCarthy (1978) and also by Gianturco and Scialla (1987) as follows

$$\int d^3 r' \varphi_a^*(\vec{r}\,') \frac{1}{|\vec{r}\,' - \vec{r}|} R_l(\vec{r}\,') \approx -\frac{4\pi}{\nabla^2} \varphi_a^*(\vec{r}) R_l(\vec{r}). \tag{3.50}$$

The exchange potential is then

$$V_{ex}u_l(r)=\frac{4\pi}{\nabla^2}\sum_{n_al_am_a}\frac{1}{r}P^2_{n_al_a}(r)u_l(r)\int d\hat{r}Y^*_{lm}(\hat{r})Y_{lm}(\hat{r})Y^*_{l_am_a}(\hat{r})Y_{l_am_a}(\hat{r}). \tag{3.51}$$

From the addition theorem of spherical harmonics (Cowan, 1981) we have

$$P_\lambda(\hat{r}_1,\hat{r}_2)=\frac{4\pi}{(2\lambda+1)}\sum_{\eta=-\lambda}^{+\lambda}Y^*_{lm}(\hat{r}_1)Y_{lm}(\hat{r}_2), \tag{3.52}$$

where P_λ is a Legendre polynomial of order λ. Consequently we have in equation (3.51)

$$\sum_{m_a=-l_a}^{l_a}\left|Y_{l_am_a}(r)\right|^2=\frac{2l_a+1}{4\pi}, \tag{3.53}$$

and therefore (3.51) becomes

$$V_{ex}u_l(r)=\frac{4\pi}{\nabla^2}\sum_{n_al_a}\frac{(2l_a+1)}{4\pi r^2}P^2_{n_al_a}(r)u_l(r), \tag{3.54}$$

so that
$$V_{ex}\nabla^2\frac{R_l(\vec{r})}{r}=2\pi\rho(r)\frac{R_l(\vec{r})}{r}, \tag{3.55}$$

where the electron charge density $\rho(r)$ of the target atom is defined as

$$\rho(r)=\sum_{n_al_a}2(2l_a+1)\frac{P^2_{n_al_a}(r)}{4\pi r^2}. \tag{3.56}$$

Now, neglecting the third term on the RHS of the radial equation (3.25) we may write the Schrödinger equation

$$\left\{\nabla^2+2\left[E'-V_{st}(r)\right]\right\}\frac{R_l(\vec{r})}{r}=2V_{ex}\frac{R_l(\vec{r})}{r}, \tag{3.57}$$

where $R_l(\vec{r})$ is defined in (3.48) and $E'=k^2/2$ is the energy of the projectile electron (in Hartrees). Using equation (3.57) in (3.55) we have

$$V^2_{ex}-V_{ex}(E'-V_{st}(r))-\pi\rho(r)=0. \tag{3.58}$$

Solving this quadratic equation yields

$$V_{ex}(r)=\frac{1}{2}\left(E'-V_{st}(r)\right)\pm\frac{1}{2}\left[\left(E'-V_{st}(r)\right)^2+4\pi\rho(r)\right]^{\frac{1}{2}}. \tag{3.59}$$

Finally choosing the physically acceptable solution to (3.59) as the one which guarantees that $V_{ex}(r)$ vanishes at high projectile energy E' we get

$$V_{ex}(r,E')=\frac{1}{2}\left\{\left(E'-V_{st}(r)\right)-\left[\left(E'-V_{st}(r)\right)^2+4\pi\rho(r)\right]^{\frac{1}{2}}\right\}. \tag{3.60}$$

This is the local exchange potential of Furness and McCarthy (1973). It is generally useful in taking into account exchange effects in elastic scattering of electrons by atoms in the intermediate to high energy region.

3.3.3 The Polarization Potential

Formal manipulation of the Lippmann-Schwinger equation (Joachain, 1975) yields the optical potential of the form (considering only the first two terms in the series expansion)

$$V_{opt}=V_{st}+\sum_{j\neq 0}\frac{\langle 0|V|j\rangle\langle j|V|0\rangle}{k^2/2-K-(\varepsilon_j-\varepsilon_0)+i\omega},\ \omega\to 0^+ \tag{3.61}$$

apart from an exchange potential.

The three-dimensional coordinate representation of the second term in (3.61), operating on the state vector of the continuum electron $|\chi\rangle$ is

$$\left\langle \vec{r}\left|\sum_{j\neq 0}\frac{\langle 0|V|j\rangle\langle j|V|0\rangle}{k^2/2-K-(\varepsilon_j-\varepsilon_0)+i\omega}\right|\chi\right\rangle$$

$$=2\sum_{j\neq 0}\int d^3r' V_{0j}G_j^+(\vec{k}_j;\vec{r},\vec{r}')V_{j0}\chi(\vec{r}') \tag{3.62}$$

where $V_{0j} = \langle 0|V|j\rangle$ and G_j^+ is the Green's function

. $$G_j^+(\vec{k}_j;\vec{r},\vec{r}') = -(2\pi)^{-3}\int d^3k' \frac{e^{i\vec{k}'.(\vec{r}'-\vec{r})}}{k'^2 - k_j^{\,2} + i\omega}. \tag{3.63}$$

In (3.63) we have defined

$$k_j = \left[k^2 + 2(\varepsilon_0 - \varepsilon_j)\right]^{\frac{1}{2}}. \tag{3.64}$$

The one-dimensional equivalent of the RHS of (3.62) is expressed as

$$2\sum_{j\neq 0}\int_0^\infty dr' V_{0j}(r) G_j{}^+(k_j;r,r') V_{j0}(r') u_l(r'),$$

where $G_j{}^+(k_j;r,r')$ is given by equation (3.24). This expression is the same as the third term on the RHS of equation (3.25). Valone *et al.* (1982) approximated the second term in (3.61) to a real, local, energy-dependent polarization potential $V_{pol}(r,E')$ of the form

$$V_{pol}(r,E') = V^{ad}/(1 - V_{se}/\Delta), \tag{3.65}$$

where $V_{se}(r,E') = V_{st}(r) + V_{ex}(r,E')$ is the static-exchange potential of the target atom, Δ is the average excitation energy of the target atom and V^{ad} is the adiabatic (energy-independent) polarization potential. Eades *et al.* (1982) calculated V^{ad} for magnesium using the extended basis set Hartree-Fock method (EBSHF). The potential is presented in table 3.1.

Table 3.1. Adiabatic polarization potential (in Hartrees) for magnesium (Eades *et al*., 1982)

r (a.u)	$V^{ad}(r)$
0.01	-2.121559
0.25	-1.038566
0.50	-0.609772
0.75	-0.339623
1.0	-0.250706
1.25	-0.209768
1.5	-0.186236
2.0	-0.160683
2.5	-0.139113
3.0	-0.115736
3.5	-0.092856
4.0	-0.072565
5.0	-0.042461
6.0	-0.024605
8.0	-0.009046
10.0	-0.003881
15.0	-0.000785
20.0	-0.000249
25.0	-0.000102
∞	0.0

3.3.4 The Absorption Potential

In order to account for the possibility of excitation and ionization of the target atom by the incident electron at intermediate energies Staszewska *et al*. (1984) proposed a quasi-free absorption potential having the form

$$V_{abs} = -\frac{1}{2} T_{loc}\left(r, E^{'}\right)\rho(r)\bar{\sigma}_b, \tag{3.66}$$

where $T_{loc}(r, E') = \left(2(E' - V_{se})\right)^{\frac{1}{2}}$ is the local kinetic energy of the incident electron, $\rho(r)$ is the electron charge density of the target atom as given by equation (3.56) and $\bar{\sigma}_b$ is the average binary collision cross section given by

$$\bar{\sigma}_b = \frac{32\pi^2 N_k}{15k^2} H(x)(f_1 + f_2). \tag{3.67}$$

In equation (3.67) $$N_k = 3/(4\pi k_F{}^3), \tag{3.68}$$

$$k_F = (3\pi^2\rho)^{\frac{1}{3}}, \tag{3.69}$$

$$f_1 = \frac{5k_F{}^3}{(\alpha - k_F{}^2)} - \frac{k_F{}^3(5(k^2-\alpha)+2k_F{}^2)}{(k^2-\alpha)^2}, \tag{3.70}$$

$$f_2 = \frac{2(2\alpha - k^2)^{\frac{5}{2}}}{(k^2-\alpha)^2} H(y), \tag{3.71}$$

and $$\alpha = (k_F{}^2 + 2\Delta). \tag{3.72}$$

In these equations k_F is the Fermi momentum and Δ is the average excitation energy of the target atom while in equations (3.67) and (3.71), *H* is the Heaviside unit step function with $x = k^2 - (2\alpha - k_F{}^2)$ and $y = 2\alpha - k^2$ respectively.

In this study a complex optical potential consisting of the static potential given by equation (3.44), the exchange potential of Furness and McCarthy (3.60), the polarization potential (3.65) and the absorption potential (3.66), has been used. This potential differs from that used by Khare *et al*. (1983) who used a real potential consisting of the static potential, a semi-empirical Buckingham-type polarization potential $V^B{}_{pol}$ and an exchange potential of the form (3.60) with V_{st} replaced by the sum $V_{st} + V^B{}_{pol}$. Yousif and Lennart (2002) used a real optical potential expressed as a sum of the static potential, a Hara exchange potential and a Hedin-Lundqvist polarization potential.

3.4 Atomic Wavefunctions

Atomic wavefunction are required for computation of the complex optical potential $V_{opt}(r,E')$ given from equations (3.27), (3.44), (3.60), (3.65) and (3.66) as

$$V_{opt}(r,E') = V_{st}(r) + V_{ex}(r,E') + V_{pol}(r,E') + iV_{abs}(r,E'). \tag{3.73}$$

In this study the analytical radial wavefunctions $P_{nl}(r)$ for magnesium calculated by Bunge *et al*. (1993) were used. These are expressed as

$$P_{nl}(r) = \sum_{j=1}^{k} c_{jn} f_{jnl}(r), \tag{3.74}$$

where $f_{jnl}(r)$ are normalized Slater-type orbitals (STOs) of the form

$$f_{jnl}(r) = \frac{\left(2\varsigma_{jnl}\right)^{I_{jn}+\frac{1}{2}}}{\left(2I_{jn}\right)!^{\frac{1}{2}}} r^{I_{jn}} \exp\left(-\varsigma_{jnl} r\right). \tag{3.75}$$

The summation in (3.74) is over *k* basis functions $f_{jnl}(r)$. In equations (3.74) and (3.75), c_{jn}, I_{jn} and ς_{jnl} denote the coefficients, integers and exponents listed in tables 3.2 and 3.3 for the $1s^2 2s^2 2p^6 3s^2\,{}^1S$ ground state of magnesium atom.

Table 3.2. 1*s*, 2*s* and 3*s* radial atomic wavefunctions for the ground state of magnesium (Bunge *et al*., 1993)

I_{js}	c_{jn}	ς_{j1s}	ς_{j2s}	ς_{j3s}
1	17.0241	0.352464	0.059265	0.016053
1	10.0727	0.481225	-0.447481	-0.096426
2	14.6751	0.198592	0.055907	0.014785
2	5.1514	0.002259	0.355163	0.077390
2	3.4870	0.000556	0.696633	0.110979
2	2.5249	-0.000136	0.058440	0.082870
3	29.9018	-0.000669	0.000283	0.000010
3	1.7568	0.000056	-0.001173	-0.232777
3	1.1659	-0.000033	0.000277	-0.494745
3	0.8244	0.000011	-0.000059	-0.37886

Table 3.3. 2*p* radial atomic wavefunction for the ground state of magnesium (Bunge *et al.*, 1993)

I_{jp}	c_{jn}	ς_{j2p}
2	14.9021	0.004178
2	6.8076	0.175692
2	4.1426	0.420054
2	2.7152	0.456246
2	1.4623	0.012155

These values are obtained from calculations based on the Hartree-Fock theory of closed-shell atoms (Cowan, 1981; Fischer *et al*., 1997; McCarthy and Weigold, 1995).

3.5 The Scattering amplitude and Cross-Sections

The radial equation (3.26) corresponds to the Schrödinger equation

$$\left\{\nabla^2 + 2\left[E' - V_{opt}(r)\right]\right\}\chi^+\left(\vec{k},\vec{r}\right) = 0\,. \tag{3.76}$$

Far away from the electron-atom interaction region, the solution to (3.76) is a superposition of a plane wave, describing the incident electron beam, and an outgoing spherical wave, describing the scattered beam. It is therefore appropriate to solve the equation subject to the boundary condition

$$\chi^+\left(\vec{k},\vec{r}\right) \underset{r\to\infty}{\longrightarrow} e^{i\vec{k}.\vec{r}} + f(\theta)\frac{e^{ikr}}{r}\,, \tag{3.77}$$

where $f(\theta)$ is the scattering amplitude.

The number of electrons scattered into a volume element $d^3r = r^2 dr d\Omega$ is

$$\left|\frac{f(\theta)}{r}e^{ikr}\right|^2 d^3r = \left|f(\theta)\right|^2 dr d\Omega\,. \tag{3.78}$$

Consequently, the number of scattered electrons $d\sigma$ entering the volume element per unit time is

$$d\sigma = |f(\theta)|^2 k d\Omega, \tag{3.79}$$

where $k = dr/dt$ is the momentum of the scattered electrons. The differential cross section, denoted by $d\sigma/d\Omega$, is defined as the number of scattered electrons entering unit solid angle per unit time per unit incident flux. The incident flux is the number of incident electrons crossing unit area per unit time and is equal to *k* for an incident plane wave (McCarthy and Weigold, 1995). The expression for the differential cross section is therefore

$$\frac{d\sigma}{d\Omega} = |f(\theta)|^2 . \tag{3.80}$$

The differential cross section (DCS) has the dimensions of area per unit solid angle and is given either in $a_o{}^2/sr$ or $10^{-20}\, m^2/sr$ units. For incident electron energy E', the DCS depends on the scattering angle θ defined as the angle between the direction of the incident electron beam and that of the detector. The integral of the DCS over all angles is the integral cross section (ICS), which is denoted by σ_I and is given by

$$\sigma_I = \int_0^{2\pi} d\phi \int_0^{\pi} d\theta \sin\theta |f(\theta)|^2 . \tag{3.81}$$

To solve the Schrödinger equation (3.76), the continuum wave function for the projectile $\chi^+(\vec{k},\vec{r})$ is expanded in terms of continuum radial wavefunctions $u_l(k,r)$ of the scattered electron and spherical harmonics

$$\chi^+(\vec{k},\vec{r}) = \sqrt{\frac{2}{\pi}} \frac{1}{kr} \sum_{l=0}^{\infty} \sum_{m=-l}^{+l} i^l u_l(k,r) Y_{lm}(\hat{r}) Y_{lm}^*(\hat{k}). \tag{3.82}$$

The radial wavefunctions satisfy the radial equation (3.26) subject to the boundary condition

$$u_l(k, r=0)=0, \tag{3.83a}$$

and

$$u_l(k, r=\infty)= j_l(\rho)-\tan\delta_l \eta_l(\rho). \tag{3.83b}$$

where $j_l(\rho)$ and $\eta_l(\rho)$ are spherical Bessel and Neumann functions respectively with argument $\rho = kr$. The complex quantity $\delta_l = a_l + ib_l$ is the phase shift corresponding to the *l*th radial wavefunction. The real and imaginary phase shifts, a_l and b_l respectively, are as a result of the distortion of $u_l(k,r)$ by the real and imaginary parts of the optical potential. Expanding the plane wavefunction in equation (3.77) in terms of Legendre polynomials $P_l(\cos\theta)$

$$e^{i\vec{k}.\vec{r}} = \sum_{l=0}^{\infty}(2l+1)i^l\, j_l(\rho)P_l(\cos\theta), \tag{3.84}$$

and using equations (3.82) and (3.83b), the condition (3.77) is satisfied if the scattering amplitude has the form (McCarthy and Weigold, 1995)

$$f(\theta)=\frac{1}{2ik}\sum_{l=0}^{\infty}(2l+1)\left(e^{2i\delta_l}-1\right)P_l(\cos\theta). \tag{3.85}$$

In the elastic electron-atom scattering problem, equation (3.26) with the optical potential given by equation (3.73) is solved numerically to obtain radial wavefunctions for l = 0, $1 \ldots l_{\max}$, where $l_{\max}$ is chosen to ensure convergence of the phase shifts ($\delta_l \to 0$ as $l \to l_{\max}$). The phase shifts are then extracted from the wavefunctions using the formula (Joachain, 1975)

$$\tan\delta_l = \frac{ks_l^{'}(ka) - \gamma_l s_l(ka)}{kc_l^{'}(ka) - \gamma_l c_l(ka)} \ . \tag{3.86}$$

In this expression $s_l = \rho j_l(\rho)$ and $c_l = \rho\eta_l(\rho)$; $\gamma_l = u_l^{-1}(d\,u_l/dr)$ is the logarithmic derivative of the numerical solution at the matching point $r = a$ (chosen to ensure that the optical potential is negligible at that point) while $s_l^{'}$ and $c_l^{'}$ are the derivatives of s_l and c_l with respect to ρ. Moreover owing to the slow convergence of the real phase shifts, the effective range formula of O'Malley *et al*. (1961) given by

$$\tan a_l = \frac{\pi\alpha_d k^2}{(2l+3)(2l+1)(2l-1)}, \tag{3.87}$$

is used to obtain these phase shifts for large-*l* values. In equation (3.87), α_d is the dipole polarizability of the target atom. The phase shifts thus obtained are used to calculate the scattering amplitude from (3.85) which in turn is used to determine differential and integral cross sections using (3.80) and (3.81).

CHAPTER 4

RESEARCH METHODS

There is no known analytical solution to the radial equation (3.26) with the optical potential given by equation (3.73). The equation is therefore solved numerically to yield $u_l(r)$ values at particular radial points on a numerical grid. In section 4.1 of this chapter, the numerical grid applied in this study is discussed. In section 4.2, the numerical quadrature rules for evaluation of static and exchange parts of the optical potential are discussed. The cubic spline method for interpolation of the magnesium adiabatic polarization potential of the Eades *et al*. (1982) is given in section 4.3. Numerov's algorithm for integrating the radial equation is presented in section 4.4. Finally, in section 4.5 the computer code for implementing the various numerical methods is discussed.

4.1 Numerical Grid

In solving differential equations numerically, choosing a numerical grid or mesh is an important first step if the solution is to be obtained accurately and efficiently. While a fine mesh with closely spaced mesh points may seem appropriate, too large an integration range will lead to accumulation of errors. The most natural grid to use is the linear mesh in which grid points are equally spaced throughout the radial integration range which is typically from $r = 0$ to $r = 80$ a.u. in atomic physics. It is known from atomic structure calculations that the radial part of bound target wave functions oscillates rapidly near the origin and decays exponentially at large radial distances. A linear mesh does not yield accurate results in this case. Instead a logarithmic grid (Fischer *et al*., 1997), in which

grid points are very close near the origin but become increasingly far apart with increasing radial distance, is more suitable. Alternatively, a Herman-Skillman mesh (Cowan, 1983) may be used. This is a linear approximation to a logarithmic grid. The mesh consists of regions of forty points with each region having equally spaced mesh points. The spacing h_1 between points in the first region is

$$h_1 = r_j - r_{j-1}, \qquad (j = 1,2,....40). \tag{4.1}$$

In the second region, the spacing h_2 is double that in the first region

$$h_2 = 2h_1 = r_j - r_{j-1}, \qquad (j = 41,42,....80). \tag{4.2}$$

The spacing h_n in the *nth* region is

$$h_n = 2^{n-1} h_1. \tag{4.3}$$

For calculation of the continuum wave functions in this study, the Herman-Skillman mesh was modified since the wave functions oscillate rapidly in the outer region of the integration range. If the occasional doubling of the spacing is continued into the outer region, the calculated continuum wave functions will be seriously in error. To avert this, the radial mesh used in this study for calculation of the wave functions of the scattered electron was an adaptation of the Herman-Skillman mesh and is similar to the one used by Bartschat (1996) for the calculation of electron elastic scattering by a hydrogen atom. Briefly, the mesh is restricted to seven regions. Each of the first five regions has forty equally spaced points; the fifth region has a hundred mesh points while the last region has twelve hundred points. The spacing in the first region is h_1. The spacing in subsequent regions is twice that of the previous region just like in the original Herman-Skillman

mesh. The integration range is from $r = 0$ to $r = 81.24$ a.u. The numerical grid is presented in table 4.1.

Table 4.1. Regions of the numerical grid

Region	Grid points	Spacing (a.u)	Start (a.u)	End (a.u)
1	40	0.001	0	0.04
2	40	0.002	0.04	0.12
3	40	0.004	0.12	0.28
4	40	0.008	0.28	0.60
5	40	0.016	0.60	0.124
6	100	0.032	0.124	4.44
7	1200	0.064	4.44	81.24

4.2 Numerical Integration

In order to evaluate the integrals in the static potential (3.44), the integrals are first written as

$$I = \int_0^{\infty} dr' \frac{P^2_{n_a l_a}(r')}{r_>} = \frac{1}{r}\int_0^{r} dr' P^2_{n_a l_a}(r') + \int_r^{r_{\max}} dr' \frac{P^2_{n_a l_a}(r')}{r'} \tag{4.4}$$

where $r_{\max}$ is set equal to about 80 a.u to ensure convergence of the infinite integral. The two resultant integrals are then evaluated using the five-point quadrature rule used by Fischer *et al*. (1997) in the evaluation of Slater integrals encountered in numerical Hartree-Fock atomic structure calculations, thus

$$I = \sum_{m=1}^{M} I_m \tag{4.5}$$

where $$I_m = \int_{x_j}^{x_{j+2}} y(x)dx$$

$$= \frac{h}{90}\left\{34\left(y_{j+2}+y_j\right)-\left(y_{j+3}+y_{j-1}\right)+114y_{j+1}\right\}+\mathrm{O}\left(h^7\right). \qquad (4.6)$$

In applying this quadrature rule the mesh points are assumed to be evenly spaced but since the rule cannot be used at the two ends of the integration range, the well known but less accurate Simpson's quadrature three-point rule is used at these points where

$$\int_{x_j}^{x_{j+2}} y(x)dx = \frac{h}{3}\left(y_j + 4y_{j+1} + y_{j+2}\right)+\mathrm{O}\left(h^5\right). \qquad (4.7)$$

Once the integrals have been evaluated the computation of the static potential (3.44), as well as the exchange potential (3.60), is straight forward.

4.3 Cubic Spline Interpolation

The adiabatic polarization potential of Eades *et al*. (1982) is given on a mesh which is different from the numerical mesh used in our study (table 3.1). In order to estimate the values of the potential on the various points of our mesh, we have used the cubic spline interpolation method (Thompson, 1992). Given *n* evenly spaced data values $y_1, y_2, ..., y_n$, the value of the function at point *x* within the range x_1 to x_n is estimated as

$$s(x) = y_j + g\left\{s_j^{(1)} + \left(s_j^{(2)}/2 + s_j^{(3)}\, g/6\right)g\right\}, \qquad (4.8)$$

where
$$g = x - x_1 - (j-1)h, \qquad (4.9)$$

and the interpolation index is

$$j = trunc\left[\left(x - x_1\right)/h\right]+1. \qquad (4.10)$$

In equations (4.9) and (4.10), *h* is the spacing of the data values. The first, second and third derivatives $s_j^{(1)}, s_j^{(2)}$ and $s_j^{(3)}$ respectively, are determined as follows:

1) the a_j coefficients are computed according to the iteration scheme

$$a_2 = 4, \qquad a_j = 4 - 1/a_{j-1}, \qquad j = 3,4,.....,n-1. \tag{4.11}$$

These spline coefficients depend only on the number of data points, *n*, and not on the data values. They could be computed and stored for reuse, provided *n* does not change.

2) With *j* increasing the first differences among the data values are computed

$$e_j = y_j - y_{j-1}, \qquad j = 2,3,.....,n. \tag{4.12}$$

and thence the second-difference quantities

$$d_2 = 6(e_3 - e_2)/h^2 - s_1^{(2)}, \tag{4.13}$$

$$d_j = 6(e_{j+1} - e_j)/h^2, \qquad j = 3,4,.....,n-2 \tag{4.14}$$

$$d_{n-1} = 6(e_n - e_{n-1})/h^2 - s_n^{(2)}, \tag{4.15}$$

and the coefficients

$$b_2 = d_2, \qquad b_j = d_j - b_{j-1}/a_{j-1}, \qquad j = 3,4,.....,n-1 \tag{4.16}$$

3) With *j* increasing, the second-derivatives are computed at the spline knots

$$s_{n-1}^{(2)} = b_{n-1}/a_{n-1}, \tag{4.17}$$

$$s_j^{(2)} = (b_j - s_{j+1}^{(2)})/a_j, \qquad j = n-2,.....,2 \tag{4.18}$$

4) Finally with j increasing, the first derivatives are determined at the knots

$$s_1^{(1)} = e_2/h - s_1^{(2)}h/3 - s_2^{(2)}h/6, \tag{4.19}$$

$$s_j^{(1)} = s_{j-1}^{(1)} - \left(s_{j-1}^{(2)} + s_j^{(2)}\right)h/2, \qquad j = 2,.....,n \tag{4.20}$$

and the third derivatives at the same points

$$s_1^{(3)} = 0, \qquad s_n^{(3)} = 0, \tag{4.21}$$

$$s_j^{(3)} = \left(s_{j+1}^{(2)} - s_j^{(2)}\right)/h, \qquad j = 2,.....,n-1 \tag{4.22}$$

4.4 The Numerov's Algorithm

In order to solve the radial equation (3.26) with the optical potential given by (3.73), Numerov's algorithm (Thompson, 1992) has been applied in this study. In general if a differential equation has the form

$$\frac{d^2y}{dr^2} = g(r)y, \tag{4.23}$$

and y is known at two points r_j and r_{j-1} on a mesh in which $r_i - r_{i-1} = h$ for all i, then the value of y at r_{j+1} is given by

$$Y_{j+1} = 2Y_j - Y_{j-1} + h^2 g_j y_j, \tag{4.24}$$

where

$$Y = y\left(1 - \frac{1}{12}h^2 g\right). \tag{4.25}$$

For the present problem

$$y(r) \equiv u_l(r), \tag{4.26}$$

and $$g(r)=\left(\frac{l(l+1)}{r^2}-k^2+2V_{opt}\right). \qquad (4.27)$$

Since the nuclear term in the optical potential (3.73) dominates in the limit $r \to 0$, the analytical solution to equation (4.23) is given to second order as (Fischer *et al*.,1997)

$$\lim_{r\to 0} y \equiv \lim_{r\to 0} u_l(r) = r^{l+1}\left(1-\frac{Zr}{l+1}\right). \qquad (4.28)$$

The first two values of the radial solution were obtained from equation (4.28). Numerov's algorithm, given by equation (4.24), was then used to propagate the numerical solution outwards. Since this algorithm assumes evenly spaced mesh points, special care was taken in applying the algorithm to the numerical grid used in this study (table 4.1). In particular, the selection of two values from the outer edge of a region on the grid for use in starting the numerical integration of the radial equation in the next region was such that the spacing between the two points was the same as that of the grid points in the next region. The integration of (3.26) yielded unnormalized solutions u_l but since it was only the phase shifts δ_l that were of interest it was not necessary to normalize the solutions.

4.5 Computer Program PSCATT

For implementation of the various numerical methods used in this study, a computer program PSCATT was written in the C programming language (Deitel and Deitel, 2004). The program takes as input the ground state atomic orbitals of a magnesium atom as tabulated by Bunge *et al*. (1993) and as given in tables 3.2 and 3.3. The output from the program is in the form of differential and integral cross sections for elastic scattering of electrons by a magnesium atom. The program is designed to solve numerically the radial

equation (3.26), with the optical potential given by equation (3.73), using Numerov's algorithm on the modified Hermann-Skillman mesh given in table 4.1. Complex phase shifts δ_l are extracted from the numerical solution, as outlined in section 3.5, for $l = 1,2,.....l_{\max}$ where $l_{\max}$ is an integer chosen to ensure convergence of the phase shifts (i.e. $\delta_l \to 0$ as $l \to l_{\max}$). The flow chart of program PSCATT is given in figure 4.1.

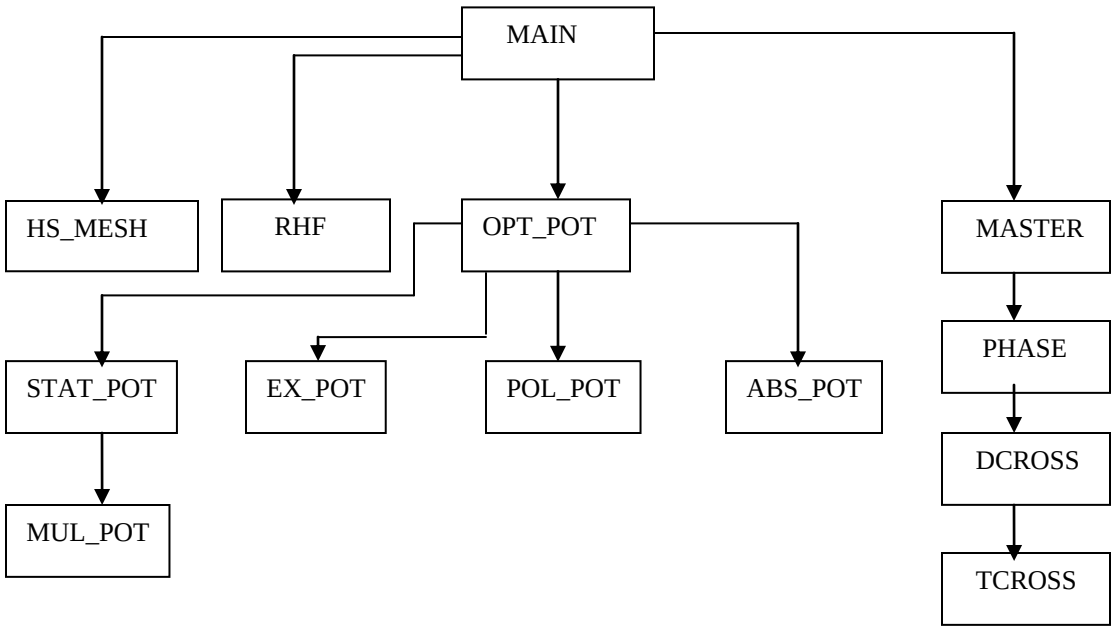

Figure 4.1 Flow chart of program PSCATT

MAIN
This is the driver function which calls functions HS_MESH, RHF, OPT_POT and MASTER.

HS_MESH
This function sets up the modified Herman-Skillman mesh given in table 4.1.

RHF
Evaluates radial atomic wave functions $P_{n_a l_a}(r)$ for magnesium according to equations (3.74) and (3.75) and as given in tables 3.2 and 3.3.

OPT_POT
Returns the optical potential equation (3.73) by calling functions STAT_POT, EX_POT, POL_POT and ABS_POT

STAT_POT
Determines the static potential as given in equation (3.44).

MUL_POT
Evaluates the integrals in equation (3.44) numerically as described in section 4.2.

EX_POT
Calculates the local exchange potential using equation (3.60).

POL_POT
Evaluates the non-adiabatic polarization potential using (3.65) based on the adiabatic potential of Eades *et al.* (1982) by application of the cubic spline interpolation method as described in section 4.3.

ABS_POT
Evaluates the absorption potential of Staszewska *et al*. (1984) as given in equations (3.66) – (3.72).

MASTER
Solves the radial Schrödinger equation (3.26) using Numerov's algorithm for an electron moving in a complex optical model potential $V_{opt}(r)$ given by equation (3.73) as described in section 4.4. Returns cross sections by calling functions PHASE, DCROSS and TCROSS.

PHASE
Extracts the phase shifts δ_l corresponding to the *l* partial wave as outlined in section 3.5.

DCROSS
Calculates the DCS using equations (3.80) and (3.85).

TCROSS
Calculates integral cross sections using equation (3.81).

CHAPTER 5

RESULTS AND DISCUSSION

In section 5.1 of this chapter the optical model potential differential cross section results for elastic scattering of electrons by a magnesium atom obtained in this study are presented. The results are compared with available experimental and calculated results. In section 5.2 the optical model potential integral cross section results are presented and compared with earlier results. The differential cross section which have dimensions of area per unit solid angle are in a_0^2 / sr units (where a_0 is the Bohr radius) and the integral cross sections are in a_0^2 units.

5.1 Differential Cross Sections

In this study differential cross sections (DCS) for elastic scattering of electrons by a magnesium atom have been calculated at 10, 15, 20, 40, 60, 80 and 100 eV for scattering angles from $\theta = 0^\circ$ to 180° using the optical model potential method. One set of the present results is obtained using a real optical potential without the absorption potential (equation 3.66) and another set is obtained using a complex optical potential including the absorption potential. In order to distinguish the present results from the optical model potential results of Khare *et al*. (1983), the present results with and without absorption are denoted by OMP3 and OMP2 respectively and the results of Khare *et al*. (1983) by OMP1. The present DCS results are listed in tables 5.1 and 5.2. In figures 5.1-7 these results are compared with the measured results of Predojevic *et al.* (2007) and of Williams and Trajmar (1978) which are denoted as EXPT1 and EXPT2 respectively. The

results are also compared with the five-state close coupling (CC5) results of Mitroy and McCarthy (1989), the convergent close coupling (CCC) results of Brown *et al.* (2003, 2005) and the optical model potential (OMP1) results of Khare *et al.* (1983).

Table 5.1 OMP2 differential cross sections for elastic scattering of electrons by a magnesium atom. (Exponential notation is used for the power of 10).

	Differential cross sections (a.u.)						
θ	10 eV	15 eV	20 eV	40 eV	60 eV	80 eV	100 eV
0	3.89E+02	4.16E+02	4.31E+02	4.64E+02	4.85E+02	5.01E+02	5.14E+02
10	1.79E+02	1.61E+02	1.46E+02	1.03E+02	8.07E+01	6.62E+01	5.58E+01
20	7.66E+01	5.68E+01	4.32E+01	1.93E+01	1.21E+01	9.10E+00	7.47E+00
30	3.11E+01	1.76E+01	1.06E+01	3.55E+00	2.87E+00	2.63E+00	2.40E+00
40	1.06E+01	3.86E+00	1.74E+00	1.34E+00	1.45E+00	1.33E+00	1.18E+00
50	2.40E+00	4.78E-01	5.69E-01	1.27E+00	1.13E+00	9.43E-01	8.01E-01
60	2.85E-01	6.97E-01	1.26E+00	1.36E+00	1.01E+00	7.61E-01	5.89E-01
70	6.33E-01	1.59E+00	1.87E+00	1.30E+00	8.29E-01	5.52E-01	3.81E-01
80	1.51E+00	2.12E+00	2.00E+00	1.05E+00	5.69E-01	3.23E-01	2.03E-01
90	2.06E+00	2.07E+00	1.68E+00	6.80E-01	2.82E-01	1.25E-01	7.05E-02
100	2.05E+00	1.60E+00	1.14E+00	3.19E-01	6.90E-02	1.07E-02	1.14E-02
110	1.62E+00	9.86E-01	6.09E-01	1.05E-01	1.77E-02	2.96E-02	5.79E-02
120	1.02E+00	4.57E-01	2.61E-01	1.37E-01	1.73E-01	2.03E-01	2.17E-01
130	4.74E-01	1.60E-01	1.84E-01	4.39E-01	5.29E-01	5.20E-01	4.80E-01
140	1.29E-01	1.29E-01	3.66E-01	9.58E-01	1.03E+00	9.39E-01	8.14E-01
150	5.49E-03	3.02E-01	7.24E-01	1.58E+00	1.59E+00	1.39E+00	1.16E+00
160	3.56E-02	5.66E-01	1.13E+00	2.18E+00	2.10E+00	1.79E+00	1.46E+00
170	1.15E-01	7.90E-01	1.44E+00	2.60E+00	2.45E+00	2.06E+00	1.67E+00
180	1.54E-01	8.64E-01	1.54E+00	2.74E+00	2.57E+00	2.16E+00	1.75E+00

From figure 5.1 it can be seen that the OMP2 results for the differential cross sections at 10 eV are in close agreement with the EXPT2 results of Williams and Trajmar (1978) for scattering angles $\leq 50^{\circ}$ but they are in little agreement at larger scattering angles. The OMP2 results are in qualitative agreement with the measured EXPT1 results of Predojevic *et al*. (2007) and are intermediate between the calculated CC5 results of

Mitroy and McCarthy (1989) and the OMP1 results of Khare *et al*. (1983). The OMP2 results are in better agreement with the measure results of Predojevic *et al*. (2007) and Williams and Trajmar (1978) than the OMP1 results of Khare *et al*. (1983) perhaps an indication that the real optical potential used in the present study is more suitable at 10 eV. The present OMP2 results have two minima at $\theta = 60^{\circ}$ and at 150° with the minimum at 60° coinciding with the minimum in measured results of Predojevic *et al*. (2007). The differential cross section is a measure of the probability of scattering in a particular direction and a minimum in the DCS results at a given angle indicates the direction in which electrons are least likely to be scattered.

Table 5.2 OMP3 differential cross sections for elastic scattering of electrons by a magnesium atom. (Exponential notation is used for the power of 10).

	Differential cross sections (a.u.)						
θ	10 eV	15 eV	20 eV	40 eV	60 eV	80 eV	100 eV
0	3.85E+02	3.89E+02	3.92E+02	4.22E+02	4.51E+02	4.72E+02	4.86E+02
10	1.78E+02	1.53E+02	1.35E+02	9.85E+01	7.96E+01	6.62E+01	5.54E+01
20	7.65E+01	5.40E+01	4.01E+01	1.80E+01	1.08E+01	7.54E+00	5.81E+00
30	3.06E+01	1.57E+01	8.65E+00	2.13E+00	1.54E+00	1.47E+00	1.48E+00
40	1.01E+01	2.76E+00	7.88E-01	5.32E-01	7.26E-01	7.87E-01	7.92E-01
50	2.13E+00	1.16E-01	2.34E-01	6.72E-01	6.60E-01	6.22E-01	5.45E-01
60	2.09E-01	5.07E-01	8.49E-01	7.67E-01	6.33E-01	5.25E-01	3.84E-01
70	5.92E-01	1.19E+00	1.18E+00	7.51E-01	5.46E-01	3.87E-01	2.34E-01
80	1.42E+00	1.50E+00	1.19E+00	6.38E-01	3.86E-01	2.26E-01	1.18E-01
90	1.92E+00	1.43E+00	1.01E+00	4.40E-01	1.96E-01	8.75E-02	3.65E-02
100	1.91E+00	1.13E+00	7.29E-01	2.24E-01	5.10E-02	6.78E-03	6.25E-03
110	1.52E+00	7.40E-01	4.44E-01	8.61E-02	1.52E-02	2.27E-02	4.47E-02
120	9.71E-01	3.94E-01	2.43E-01	1.03E-01	1.24E-01	1.49E-01	1.53E-01
130	4.64E-01	1.84E-01	1.89E-01	2.99E-01	3.72E-01	3.80E-01	3.23E-01
140	1.33E-01	1.46E-01	2.96E-01	6.43E-01	7.26E-01	6.85E-01	5.36E-01
150	6.92E-03	2.54E-01	5.27E-01	1.06E+00	1.12E+00	1.01E+00	7.51E-01
160	2.85E-02	4.35E-01	7.98E-01	1.46E+00	1.48E+00	1.30E+00	9.36E-01
170	9.98E-02	5.94E-01	1.01E+00	1.74E+00	1.72E+00	1.50E+00	1.07E+00
180	1.36E-01	6.45E-01	1.08E+00	1.84E+00	1.80E+00	1.57E+00	1.11E+00

Figure 5.1 shows that the OMP2 and OMP3 results are virtually the same implying that the effect of the absorption potential at 10 eV is negligible.

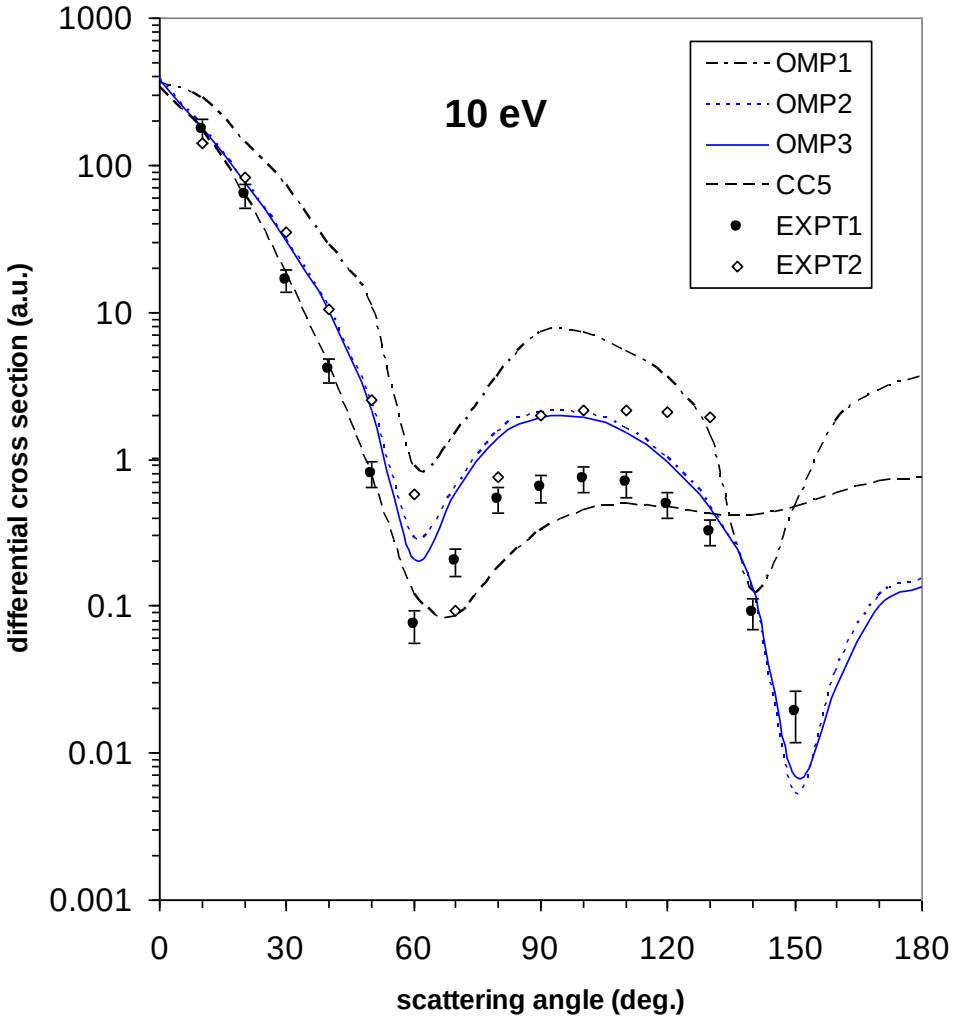

Figure 5.1 Differential cross sections for elastic scattering of electrons by magnesium atom at 10 eV incident energy. Experimental data: EXPT1, Predojevic *et al*. (2007); EXPT2, Williams and Trajmar (1978). Calculations: OMP1, optical model potential (Khare *et al*., 1983); OMP2, present optical model potential without absorption; OMP3, present optical model potential with absorption; CC5, five-state close coupling (Mitroy and McCarthy, 1989).

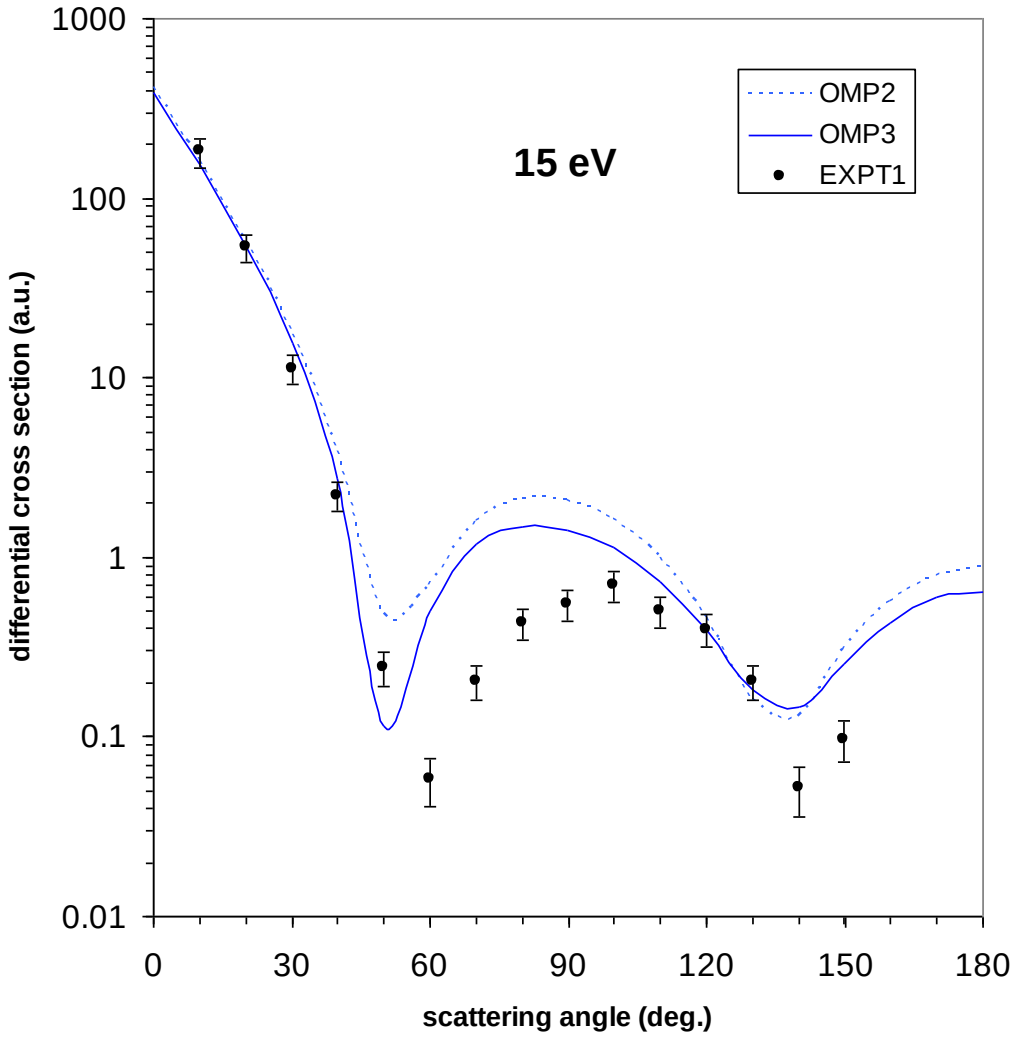

Figure 5.2 Differential cross sections for elastic scattering of electrons by magnesium atom at 15 eV incident energy. Experimental data: EXPT1, Predojevic *et al*. (2007). Calculations: OMP2, present optical model potential without absorption; OMP3, present optical model potential with absorption.

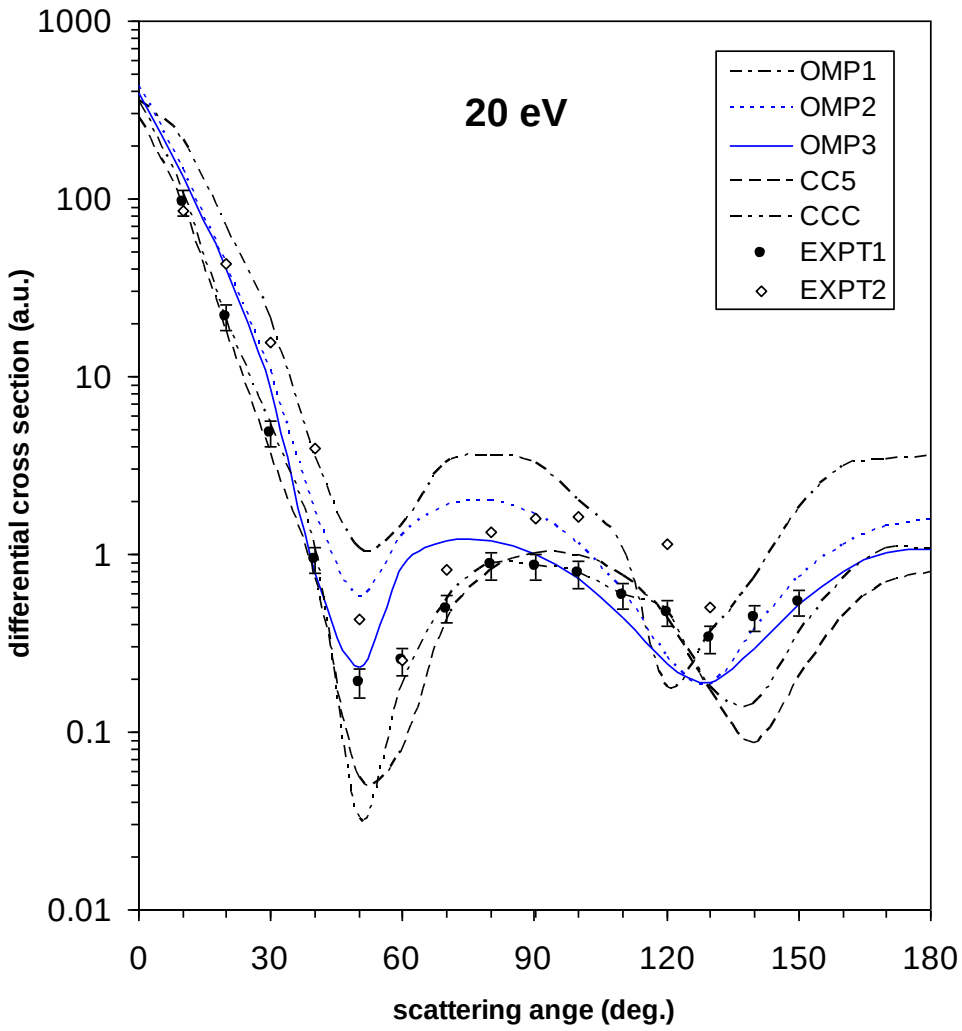

Figure 5.3 Differential cross sections for elastic scattering of electrons by magnesium atom at 20 eV incident energy. Experimental data: EXPT1, Predojevic *et al*. (2007); EXPT2, Williams and Trajmar (1978). Calculations: OMP1, optical model potential (Khare *et al*., 1983); OMP2, present optical model potential without absorption; OMP3, present optical model potential with absorption; CC5, five-state close coupling (Mitroy and McCarthy, 1989); CCC, convergent close coupling of (Brown *et al.*, 2005).

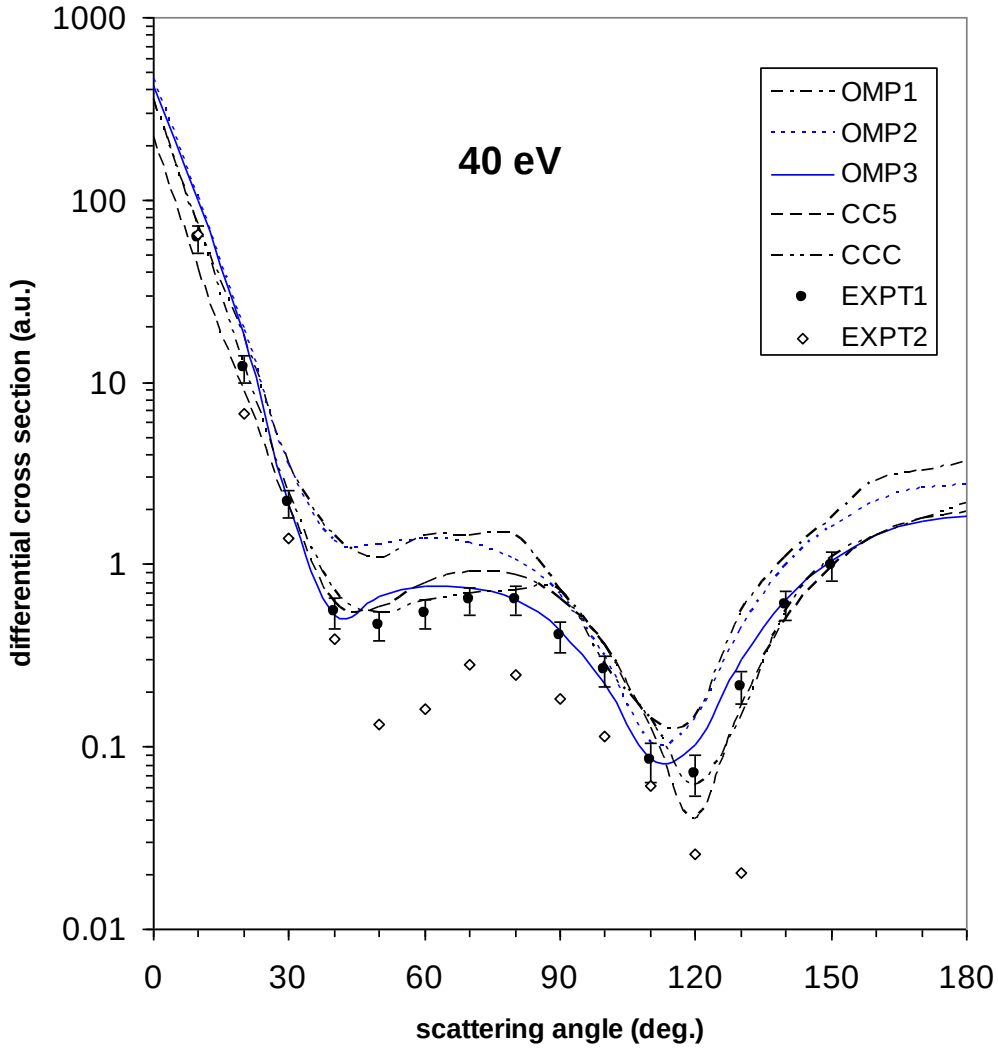

Figure 5.4 Differential cross sections for elastic scattering of electrons by magnesium atom at 40 eV incident energy. Experimental data: EXPT1, Predojevic *et al*. (2007); EXPT2, Williams and Trajmar (1978). Calculations: OMP1, optical model potential (Khare *et al*., 1983); OMP2, present optical model potential without absorption; OMP3, present optical model potential with absorption; CC5, five-state close coupling (Mitroy and McCarthy, 1989); CCC, convergent close coupling of (Brown *et al*., 2003).

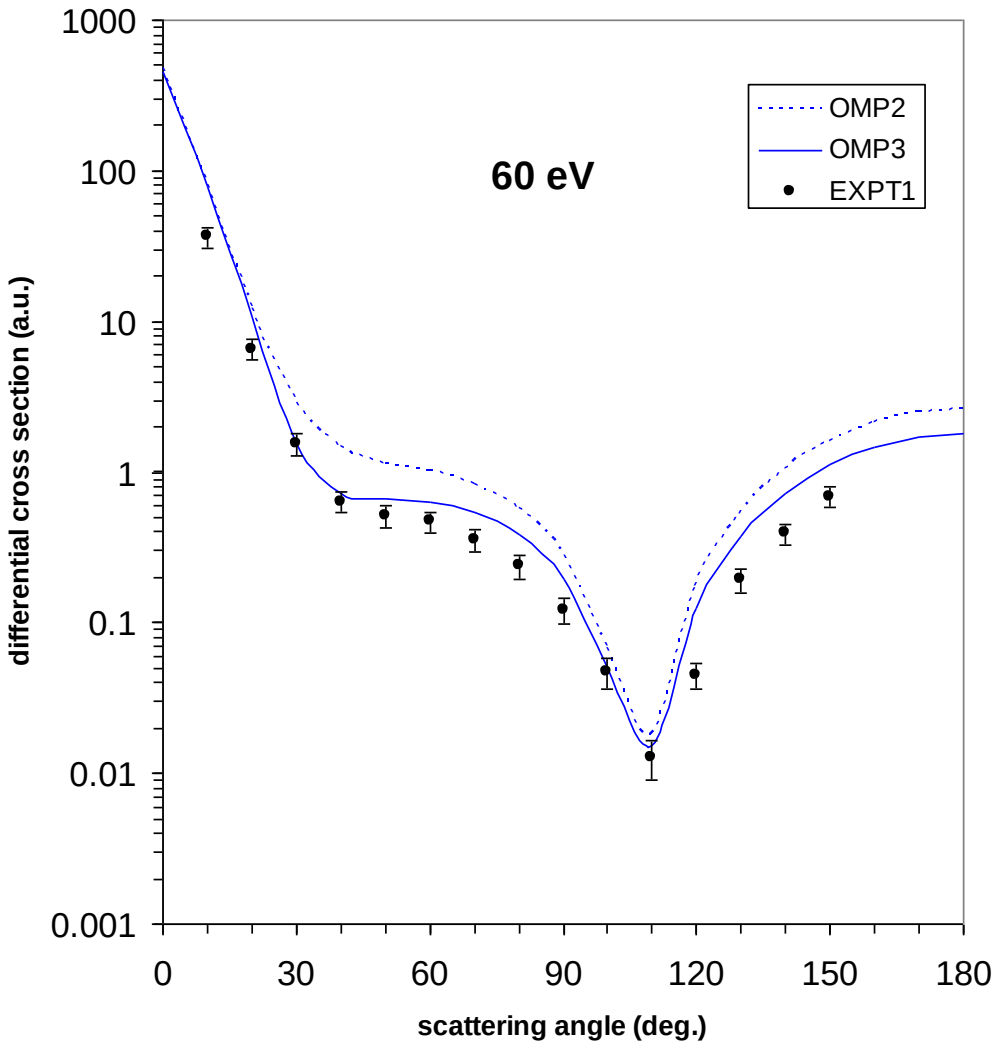

Figure 5.5 Differential cross sections for elastic scattering of electrons by magnesium atom at 60 eV incident energy. Experimental data: EXPT1, Predojevic *et al*. (2007). Calculations: OMP2, present optical model potential without absorption; OMP3, present optical model potential with absorption.

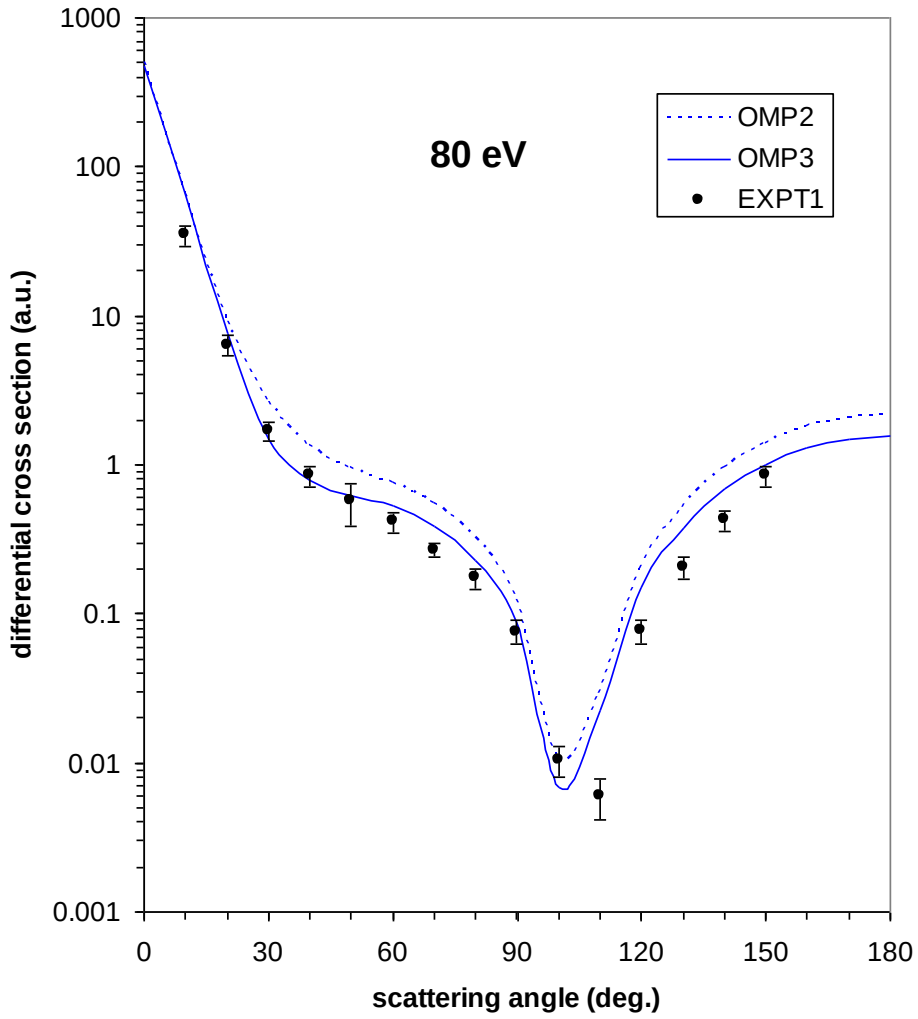

Figure 5.6 Differential cross sections for elastic scattering of electrons by magnesium atom at 80 eV incident energy. Experimental data: EXPT1, Predojevic *et al*. (2007). Calculations: OMP2, present optical model potential without absorption; OMP3, present optical model potential with absorption.

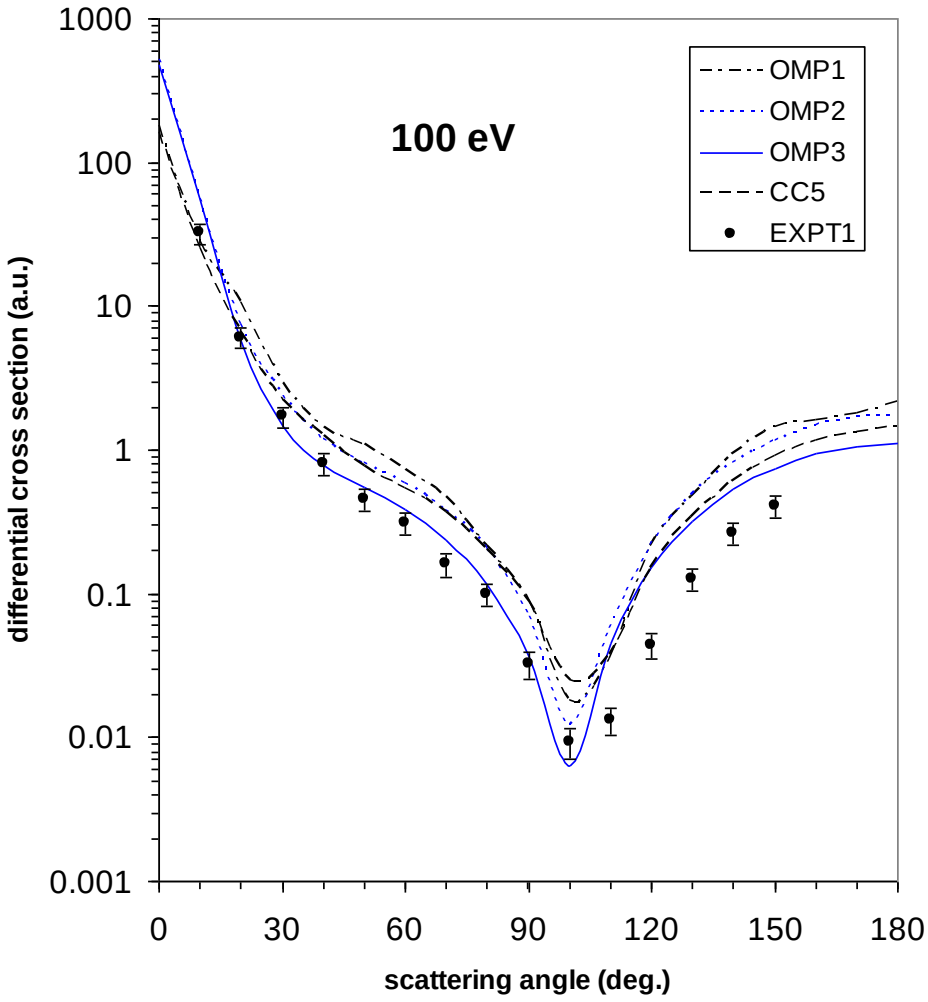

Figure 5.7 Differential cross sections for elastic scattering of electrons by magnesium atom at 100 eV incident energy. Experimental data: EXPT1, Predojevic *et al*. (2007). Calculations: OMP1, optical model potential (Khare *et al*., 1983); OMP2, present optical model potential without absorption; OMP3, present optical model potential with absorption; CC5, five-state close coupling (Mitroy and McCarthy, 1989).

The real part of the optical potential is therefore seen to dominate at 10 eV. This implies that to get better agreement with the measured results of Predojevic *et al*. (2007) and the calculated results of Mitroy and McCarthy (1989), the real part of the optical potential should be improved. In particular since exchange effects are most important at energies slightly above the ionization potential of target (about 7.4 eV for magnesium) it is likely that use of an *ab initio* exchange potential, which involves treating the second integral in equation (3.49) exactly, would yield better results.

From figure 5.2 it can be seen that at 15 eV the OMP2 results exhibit good agreement with the measured results of Predojevic *et al.* (2007) at small scattering angles up to $\theta = 50^{\circ}$. This implies that the polarization potential (equation 3.65) used in the present study is adequate at energies near the ionization threshold. This is the case since the polarization potential is the long-range part of the optical potential and dominates small angle scattering. Classically this may be understood by noting that the electrons scattered the least pass far away from the atomic charge cloud and mainly experience this part of the optical potential. At intermediate and large scattering angles the OMP2 results are generally higher than the results of Predojevic *et al*. (2007). Agreement between the OMP2 and EXPT1 results would probably be improved by use of an *ab initio* exchange potential. The present OMP3 results show that at 15 eV the absorption potential has the significant effect of reducing the DCS results particularly at scattering angles $\geq 30^{\circ}$. In the intermediate energy region (10 – 100 eV), it is well known that a real potential, such as the potential used in the present OMP2 calculation and in the OMP1 calculation of Khare *et al*. (1983), yields elastic scattering DCS results that are systematically higher

than measured results (Joachain, 1975). For accurate DCS a complex potential is needed to account for removal of incident electrons from the elastic channel. In this energy region a significant proportion of incident electrons excites and ionizes the target atoms losing energy in the process. These inelastically scattered electrons are not measured in experimental set-ups designed to only detect elastically scattered electrons. This explains why the OMP3 results at 15 eV are lower than the OMP2 results. There are no other experimental or calculated DCS results at 15 eV to compare with the OMP2 and OMP3 results, apart from the results of Predojevic *et al.* (2009), which is also the case at 60 and 80 eV.

At 20 eV figure 5.3 shows that the OMP2 results are close to the EXPT2 results of Williams and Trajmar (1978) and the EXPT1 results of Predojevic *et al*. (2007) for small scattering angles up to $\theta = 40^\circ$. The OMP2 results have two minima at $\theta = 50^\circ$ and at 130° coinciding with the minima in the measured EXPT1 results. The OMP2 results are significantly lower than the OMP1 results of Khare *et al.* (1983) at practically all scattering angles but are higher than both the CC5 results of Mitroy and McCarthy (1989) and the CCC results of Brown *et al*. (2005). However while the CC5 and CCC calculations both have two minima, these are much deeper and only the first minimum at $\theta = 50^\circ$ coincides with the minima in the EXPT1 results. At 20 eV the OMP3 results again indicate that inclusion of the absorption potential yields results that are in better agreement with the EXPT1 results at intermediate angles $\left(30^\circ \le \theta \le 100^\circ\right)$.

Figure 5.4 for incident energy 40 eV shows that the present OMP3 results are in very close agreement with the measured EXPT1 results of Predojevic *et al*. (2007) at scattering angles $\geq 20^{\circ}$ and are significantly higher than the EXPT2 results of Williams and Trajmar (1978). The OMP3 results are in reasonable agreement with the CC5 results of Mitroy and McCarthy (1989) and with the CCC results of Brown *et al*. (2003). Both the CC5 and CCC are multi-channel methods which involve explicit use of excited target states as well as the ground state. That the relatively simple optical model potential method yields results that are comparable to these sophisticated methods is remarkable. The OMP2 differential cross section results are higher than the EXPT1 results of Predojevic *et al.* (2007) and than the EXPT2 results of Williams and Trajmar (1978) but are in very good agreement with the OMP1 results of Khare *et al*. (1983) which also uses a real potential. The OMP2 results are higher than the CC5 results of Mitroy and McCarthy (1989) as well as the CCC results of Brown *et al*. (2003). This is as expected since the OMP2 results were obtained without an absorption potential.

In figures 5.5 and 5.6 it can be seen that the OMP2 results are in good qualitative agreement with the EXPT1 results of Predojevic *et al*. (2007) at 60 and 80 eV. At 60 eV, the minimum in the DCS results is at $\theta = 110^{\circ}$ for both the calculated OMP2 and measured EXPT1 results. However, at 80 eV the OMP2 results have a minimum at $\theta = 100^{\circ}$ whereas the minimum in the EXPT1 results is at $\theta = 110^{\circ}$. The present OMP3 results are in very good agreement with the EXPT1 results at scattering angles $\geq 20^{\circ}$. However the OMP3 and OMP2 results are higher than the results of Predojevic *et al*. (2007) at small scattering angles $< 20^{\circ}$. This implies that the present polarization

potential (equation 3.65), which affects small – angle scattering significantly, is not very appropriate at the higher end of the intermediate energy range.

Finally, at 100 eV figure 5.7 shows that the OMP2 results are in close agreement with the measured results of Predojevic *et al.* (2007) and also with the OMP1 and CC5 results of Khare *et al*. (1983) and Mitroy and McCarthy (1989) respectively. The present OMP3 results give the best agreement with the measured EXPT2 results especially at intermediate scattering angles $\left(20^{\circ} \le \theta \le 100^{\circ}\right)$. This is as expected since the OMP1 and OMP2 calculations involved real potentials and the CC5 calculation was limited to a few excited states neglecting the ionization channel (Mitroy and McCarthy, 1989).

In summary it can be seen from figures 5.1 – 7 that the present OMP2 results obtained without absorption are in reasonably good agreement with the recent EXPT1 results of Predojevic *et al.* (2007). The OMP2 differential cross section results are better than the OMP1 results of Khare *et al*. (1983) as compared to the EXPT1 results of Predojevic *et al.* (2007) at 10 and 20 eV. This is not surprising since as noted by Khare *et al*. (1983), the polarization potential used in the OMP1 calculations is not valid at incident energies slightly above the ionization energy of the magnesium atom which is about 7.4 eV (Predojevic *et al*., 2007). The OMP3 results, obtained with the absorption potential included in the optical potential, are in better agreement with the EXPT1 results than the OMP1 and OMP2 results. The OMP3 results are comparable to the CC5 and CCC results and are in better agreement with the EXPT1 results than these multi – channel methods at 20 and 100 eV.

5.2 Integral Cross Sections

In this study integral cross sections (ICS) for elastic scattering of electrons by a magnesium atom were calculated at 10 – 100 eV. Table 5.2 gives the present elastic integral cross sections, obtained using real and complex potentials and denoted by OMP2 and OMP3 respectively, as well as the OMP1 results of Khare *et al*. (1983), the CC5 results of Mitroy and McCarthy (1989), the EXPT1 results of Predojevic *et al*. (2007) and the EXPT2 results of Williams and Trajmar (1978). These results are also compared in figure 5.8.

Table 5.3 OMP2 and OMP3 integral cross sections for elastic scattering of electrons by a magnesium atom.

	Integral cross sections (a.u.)					
E (eV)	OMP1	OMP2	OMP3	CC5	EXPT1	EXPT2
10	198.7	105.7	103.9	79.1	81.9	103.6
15		82.3	74.1		73.6	
20	104.8	69.4	59.4	37.7	41.8	57.1
40	35.6	46.4	39.4	23.7	28.1	23.6
60		37.9	32.1		16.5	
80		31.4	27.7		16.1	
100	17.2	27.5	23.9	15.7	14.3	

Figure 5.8 shows that the OMP2 integral cross section results are in good agreement with other calculated and measured ICS at energies slightly above the ionization threshold but at higher energies the OMP2 results are systematically higher than other results. These discrepancies indicate that the OMP2 results have been obtained using a polarization potential that is too attractive at energies near the upper limit of the intermediate energy region (at 100 eV). This is so because the long-range polarization potential is known to significantly affect the differential cross sections at small angles $\left(\theta \leq 10^{\circ}\right)$ and it is exactly from these angles that we have the main contribution to the integral cross section

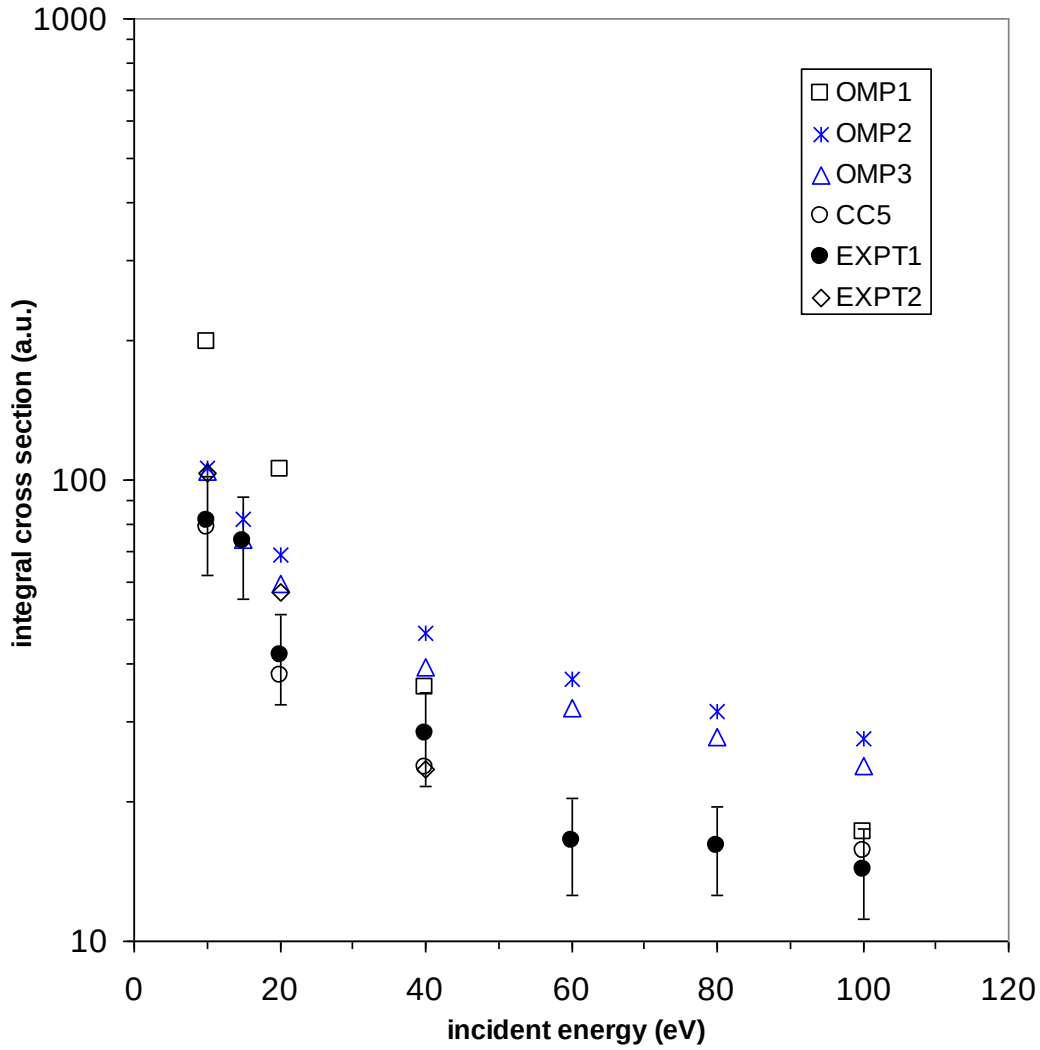

Figure 5.8. Integral cross sections for elastic scattering of electrons by magnesium atom. Experimental data: EXPT1, Predojevic *et al*. (2007); EXPT2, Williams and Trajmar (1978). Calculations: OMP1, optical model potential (Khare *et al*., 1983); OMP2, present optical model potential without absorption; OMP3, present optical model potential with absorption; CC5, five-state close coupling (Mitroy and McCarthy, 1989).

which is calculated from the differential cross sections according to equation (3.81). For this reason it would seem that to improve the OMP2 integral cross section results, the polarization potential given in equation (3.65) needs to be reconsidered. In particular since equation (3.65) is obtained approximately from the second term in equation (3.61), it may be necessary to evaluate the second term either by involving some of the infinite number of excited target states in the summation explicitly or by closure (Joachain, 1975). The OMP3 integral cross section results are lower than the OMP2 results. This is as expected since inclusion of absorption lowers elastic differential cross sections resulting in reduced integral cross sections.

CHAPTER 6

CONCLUSIONS AND RECOMMENDATIONS

In this study differential and integral cross sections for elastic scattering of electrons by a magnesium atom at intermediate energies were calculated using a complex optical potential. This chapter presents important conclusions and recommendations based on the results of the study.

6.1 Conclusions

The following conclusions are made:

- From this study it is evident that a complex optical potential incorporating an absorption potential, which accounts for the possibility of excitation and ionization of the magnesium atom by the incident electrons at intermediate energies, is crucial in obtaining good agreement with measured DCS. The use of a real optical potential at these energies is not sufficient and produces results that are significantly higher than measured results.

- The optical model potential method yields differential cross section results for electron-magnesium elastic scattering at intermediate energies that are generally better than the results obtained using (sophisticated, computationally expensive) multi-channel methods such as the convergent-close-coupling method. This implies that correlation effects are not important in elastic electron-atom scattering and therefore the use of a single Slater determinant atomic

wavefunction (as in the Hartree-Fock method) to describe the ground state of the target atom is justified in the calculation of the optical potential as opposed to use of a linear combination of Slater determinants (as in the multi-configuration Hartree-Fock, MCHF, and the configuration interaction, CI, method). This is particularly important for magnesium atom which has an open-shell structure and for which inclusion of correlation effects is considered to be necessary in the description of the ground state (Cowan, 1983; Fischer *et al*. 1997; McCarthy and Weigold, 1995).

- At incident electron energies just above the ionization threshold (10 – 20 eV), the polarization potential used in this study is well suited for calculation of small-angle DCS and of ICS for the elastic scattering of electrons by magnesium atom. At greater energies the present polarization potential yields results that are significantly higher than other calculated and measured results.

- Near the ionization threshold (10 – 20 eV), the approximate exchange potential used in this study is not accurate in the calculation of DCS for elastic scattering of electrons by magnesium atom and leads to results that are significantly higher than measured results.

6.2 Recommendations

The optical model potential method is capable of yielding good results for elastic electron-magnesium scattering at intermediate energies. The following recommendations, based on the findings of this study, are made to improve the method:

- A polarization potential that could yield better small-angle DCS and ICS results than the potential used in this study and than the semi-empirical potential of Khare *et al*. (1983) for magnesium, over the entire intermediate-energy range, should be formulated. A method that may prove successful is one based on the evaluation of the second-order term in the optical potential by closure (Joachain, 1975). Such an approach could possibly produce an accurate polarization potential without the need to use excited target states.

- An *ab initio* exchange potential should be incorporated in the optical potential, in place of the approximate exchange potential use in this study, by treating equation (3.49) exactly. This could have a significant effect on the DCS near the ionization threshold where exchange effects are most important.

REFERENCES

Bartschat, K. (1996). In *Computational Atomic Physics: Electron and Positron Collisions with Atoms and Ions*, ed. Bartschat, K. (Springer-Verlag, Berlin). Pp 10-12.

Bartschat, K., McEachran, R.P. and Stauffer, A.D. (1988). Optical Potential Approach to Electron and Positron Scattering from Noble Gases: I. Argon. *J. Phys. B* **21**, 2789-2800.

Brown, D.O., Crowe, A., Fursa, D.V., Bray, I. and Bartschat, K. (2005). Electron Scattering from Magnesium at an Incident Energy of 20 eV. *J. Phys. B* **38,** 4123 – 4134.

Brown, D.O., Cvejanovic, D. and Crowe, A. (2003). Scattering of 40 eV Electrons from Magnesium: A Polarization Correlation Study for the 3^1P state and Differential Cross Sections for Elastic Scattering and Excitation of the 3^1P and 3^3P state. *J. Phys. B* **36,** 3411 – 3423.

Bunge, C.F., Barrientos, J.A. and Bunge, A.V. (1993). Roothaan-Hartree-Fock Ground-state Atomic Wave Functions: Slater-Type-Orbital Expansions and Expectation Values for $Z = 2 - 54$ *Atomic Data and Nuclear Data Tables* **53**, 113 – 401.

Burke, P.G. and Berrington, K.A. (1993). In *Atomic and Molecular Processes: An R-Matrix Approach.* (IoP, Bristol) pp 3 – 15.

Chattopadhyay, P. (1990). In *Mathematical Physics*. (New Age International, New Dehli). Pg 177.

Cowan, R.D. (1981). In *The Theory of Atomic Structure and Spectra*.(University of California Press, Berkeley). pg 178.

Deitel, H.M. and Deitel, P.J. (2004). In *C: How to Program*. (Prentice-Hall Inc, New Jersey). pp 1 - 233.

Eades, R.A., Dixon, D.A. and Truhlar, D.G. (1982). Ab initio Adiabatic Polarisation Potentials for Be and Mg. *J. Phys. B* **15**, 3365 - 3375.

Fischer, C.F., Brange, T. and Jonsson, P. (1997). In *Computational Atomic Structure*, (IoP, London). pp 1 – 63.

Furness, J.B. and McCarthy, I.E. (1973). Semiphenomenological Optical Model for Electron Scattering on Atoms. *J. Phys. B.* **6**, 2280 - 2291.

Gianturco, F.A. and Scialla, S. (1987). Local Approximations of Exchange Interaction in Electron-Molecule Collisions: the Methane Molecule. *J. Phys. B.* **20**, 3171 – 3189.

Joachain, C.J. (1975). In *Quantum Collision Theory*. (North-Holland, Amsterdam). pp 576 – 621.

Jabloski, A., Salvat, F. and Powell, C.J. (2004). Comparison of Electron-Elastic-Scattering Cross Sections Calculated from Two Commonly used Atomic Potentials. *J. Phys. Chem.* **33,** 409- 451.

Khare, S.P., Kumar, A. and Kusum, L. (1983). Elastic Scattering of Electrons and Positrons by Magnesium Atoms at Intermediate Energies. *J. Phys. B* **16**, 4419 - 4426.

McCarthy, I.E., Ratnavelu, K. and Zhou, Y. (1989). Coupled-Channels Optical Calculation of Electron-Magnesium Scattering. *J. Phys. B* **22**, 2597 - 2603.

McCarthy, I.E. and Weigold, E. (1995). In *Electron-Atom Collisions*. (Cambridge University Press, Cambridge). pp 156 – 190.

McEachran, R.P. (1996). In *Computational Atomic Physics: Electron and Positron Collisions with Atoms and Ions*, ed. Bartschat, K. (Springer-Verlag, Berlin). Pp 102-109.

Mitroy, J. and McCarthy, I.E. (1989). Differential Cross Sections and Stokes Parameters for Electron-Magnesium Scattering. *J. Phys. B* **22**, 641 - 654.

O'Malley, T.F., Spruch, L. and Rosenberg, L. (1961). Modification of Effective-Range Theory in the Presence of a Long-Range $\left(r^{-4}\right)$ Potential. *J. Math. Phys*. **2**, 491 - 502.

Predojevic, B., Pejcev, V., Filipovic, D.M., Sevic, D. and Marinlovic, B.P. (2007). Elastic Electron Scattering by a Magnesium Atom. *J. Phys. B* **40,** 1853 – 1861.

Staszewska, G., Schwenke, D.W. and Truhlar, D.G. (1984). Investigation of the Shape of the Imaginary part of the Optical-Model Potential for Electron Scattering by Rare Gases. *Phys. Rev. A* **29**, 3078 – 3091.

Thompson, W.J. (1992). In *Computing for Scientists and Engineers*. (John Wiley and Sons Ltd, New York). pp 201 – 240.

Valone, S.M., Truhlar, D.G. and Thirumalai, D. (1982). Localized Second-Order Optical Potential for Electron Scattering in terms of Imaginary-Frequency Susceptibilities. *Phys. Rev. A* **25**, 3003 -3014.

Vanderpoorten, R. (1975). A Local Optical Potential Study of Elastic Electron-Atom Scattering. *J. Phys. B* **8**, 926 - 939.

Williams, W. and Trajmar, S. (1978). Electron Impact Excitation of Magnesium at 10, 20, and 40 eV Impact Energies. *J. Phys. B* **11**, 2021 - 2029.

Yousif, S.Y. and Lennart, J. (2002). Local-Density Approximations to the Elastic Scattering of Electrons from Mg and Ba Atoms. *Physica Scripta* **65**, 387 - 391.